

Energy Harvesting Through Reverse Electrowetting

Rohit Shrivastava

A Dissertation Submitted to
Indian Institute of Technology Hyderabad
In Partial Fulfillment of the Requirements for
The Degree of Master of Technology



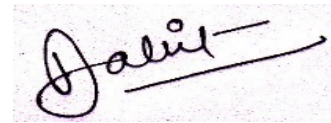
भारतीय प्रौद्योगिकी संस्थान हैदराबाद
Indian Institute of Technology Hyderabad

Department of Electrical Engineering

June, 2014

Declaration

I declare that this written submission represents my ideas in my own words, and where others' ideas or words have been included, I have adequately cited and referenced the original sources. I also declare that I have adhered to all principles of academic honesty and integrity and have not misrepresented or fabricated or falsified any idea/data/fact/source in my submission. I understand that any violation of the above will be a cause for disciplinary action by the Institute and can also evoke penal action from the sources that have thus not been properly cited, or from whom proper permission has not been taken when needed.




(Signature)

(Rohit Shrivastava)

(EE11M12)

Approval Sheet

This thesis entitled Energy harvesting through Reverse Electrowetting by Rohit Shrivastava is approved for the degree of Master of Technology from IIT Hyderabad.



Examiner



Examiner



Adviser



Co-Adviser



Chairman

Acknowledgements

First of all I want to acknowledge Dr. Shiv Govind Singh sir for his consistent guidance, support and help. All the transparent discussions and philosophies were very helpful to me.

I am willing to thank Dr. Asudeb Dutta sir and Dr. Siva Rama Krishna sir for helping me with their research experience.

I am also grateful to Tamal bhैया and Durga bhैया for helping me through out in my project.

I want to express my gratitude towards Dr. Rahul Shukla sir (Scientific officer, RRCAT) for his guidance and support. I am taking this opportunity to acknowledge my friends Akshita for helping me in X-ray mask making, Ankit for helping me in PMMA bonding, Harry for helping me in alignment and Sangram for CAD drawing.

Finally, I want to thank my friends Manas, Ghanashyam, Nagveni, Meher, Jitendra, Raman, Pramod, Roopak and Bala for making my stay in IITH so special and wonderful.

To my family & friends...

Abstract

Over the last decade electrical batteries have emerged as a critical bottleneck for portable electronics development. High-power mechanical energy harvesting can potentially provide a valuable alternative to the use of batteries, but, until now, a suitable mechanical-to-electrical energy conversion technology did not exist. Here we describe a novel mechanical-to-electrical energy conversion method based on the reverse electrowetting phenomenon. Reverse electrowetting has emerged as a highly potential method for high power energy harvesting with good environmental coupling. Device simulation using fluid flow model of COMSOL multiphysics has been presented in this thesis. Harvested energy from this kind of device is directly proportional to change in capacitance from wetting to non-wetting condition i.e. the device should have high capacitance per unit volume. It has been found that high K dielectric material offers high capacitance at low operating voltage. Further reduction in operating voltage can be accomplished by decreasing dielectric thickness. However it has been proposed to use 10nm dielectric thickness for ease in fabrication. Finally capacitance of 4.213nF at an operating voltage of 4.9V has been achieved by choosing 10nm of TiO₂ ($\epsilon_r = 80$) as a dielectric material with the device of radius 100um. Instead of using single big droplet, use of multiple small droplets of same volume offer more capacitance and hence the harvested energy.

Apart from this simulation, device fabrication has been done using two different methods, one is based on UV lithography and another is based on X-ray lithography. All the obstacles and problems encountered in this fabrication have been discussed thoroughly in this thesis.

Abbreviations

PPR: Positive photo-resist

UV: Ultraviolet

SS: Stainless steel

PMMA: Poly methyl methacrylate

EWOD: Electrowetting on dielectric

DI: De-ionized

HMDS: Hexamethyldisilazane

IPA: Isopropanol Alcohol

Content

Declaration	ii
Approval Sheet	iii
Acknowledgements	iv
Abstract	vi
Abbreviations	vii
Chapter1: Introduction	1
Chapter2: Principle & device operation	3
Chapter3: Device simulation	7
Chapter4: Device fabrication using deep X-ray lithography	13
4.1: X-ray Mask fabrication	13
4.2: Process flow of Reverse-electrowetting based energy harvester	14
Chapter5: Device fabrication using UV lithography with Positive photoresist	19
5.1: Process flow of Reverse-electrowetting based energy harvester	19
Chapter6: Device fabrication using UV lithography with SU-8	24
6.1: Process flow of Reverse-electrowetting based energy harvester	24
6.2: Isometric view of the energy harvester	29
Chapter7: Device fabrication without electroplating	30
7.1: Process flow of Reverse-electrowetting based energy harvester	30
7.2: Isometric view of the energy harvester	33
Chapter8: Implementation	34
8.1: Device fabrication using deep X-ray lithography	34
8.1.1: X-ray Mask fabrication	34
8.1.2: Reverse electrowetting based energy harvester fabrication.	38
8.2: Device fabrication using UV lithography with Positive photoresist	45
8.3: Device fabrication using UV lithography with SU-8	51
8.4: Device fabrication without electroplating	54
Conclusion & future work	58
References	59

Chapter1

Introduction

Over the last decade electrical batteries have emerged as a critical bottleneck for the portable electronics development. High-power mechanical energy harvesting can potentially provide a valuable alternative to use of batteries, but until now a suitable mechanical-to-electrical energy conversion method technology did not exist. Here a novel Mechanical to electrical energy conversion method based on reverse electrowetting phenomenon has been described. Energy generation is achieved through the interaction of arrays of moving microscopic liquid droplets with a novel multilayer thin film [1]. Advantages of this method are the production of high power density up to $1\text{KW}/\text{m}^3$ (much higher as compare to other harvester) and excellent environmental coupling. Environment is enormous source of vibrations, even in normal walking we lose around $7\text{W}-10\text{W}$ of power in the form of heat. So we can utilize this Mechanical energy and deliver power to cell-phones or Microcomputers which are working below 10W .

Table1: Power Density of different Energy harvesters:

Energy Source	Harvested Power density
Vibration/Motion	
Human	4 $\mu\text{W}/\text{cm}^2$
Industry	100 $\mu\text{W}/\text{cm}^2$
Temperature Difference	
Human	25 $\mu\text{W}/\text{cm}^2$
Industry	1–10 mW/cm^2
Light	
Indoor	10 $\mu\text{W}/\text{cm}^2$
Outdoor	10 mW/cm^2
RF	
GSM	0.1 $\mu\text{W}/\text{cm}^2$
WiFi	0.001 mW/cm^2
Reverse electrowetting based	100m W/cm²

Chapter2

Device principle and operation

In the recent years, electrowetting on dielectric (EWOD) showed numerous applications from fluid separation to high power energy harvesting. Electrowetting is nothing but controlling the wettability of dielectric surface by electric potential [2] as shown in *Fig.1*. The wettability change arises from the extra electrostatic energy associated with liquid-solid interface when the external source applied between conductive droplet and the dielectric-film-coated electrode [2]. The degree of wettability is governed by [2],

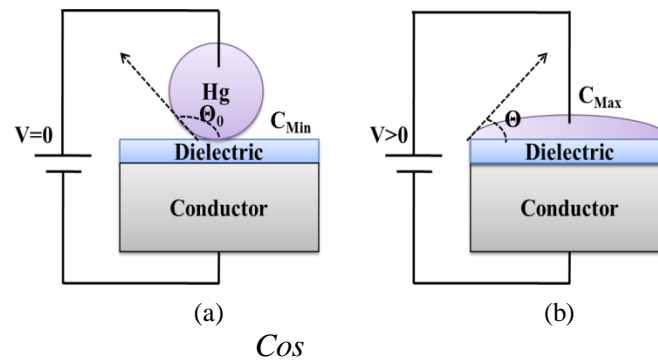


Fig.1.Electrowetting on dielectric (a) At $V=0$; (b) At $V>0$.

$$\cos\theta = \cos\theta_0 + \frac{\epsilon_0\epsilon_r}{2 * \gamma * d} V^2$$

Here,

θ =Instantaneous contact angle,

θ_0 =Contact angle at zero biasing, \cos

ϵ_0 =Electric permittivity= $8.854 * 10^{-12}$ F/m,

ϵ_r =Dielectric constant,
 V =Applied voltage,
 γ =Interfacial tension,
 d =Dielectric thickness.

On the application of applied voltage, solid-liquid interfacial energy decreases, which leads in spreading of the liquid onto the solid therefore the Solid-liquid interfacial area increases results in increase in capacitance [2]. The Lippmann's effective solid-liquid interfacial energy is [2],

$$\gamma_{sleff} = \gamma_{slo} - \frac{CV^2}{2}$$

Here,

γ_{slo} = Solid-liquid interfacial energy at zero bias,
 C =Capacitance per unit area of the interface,
 V =Applied voltage.

In electrowetting, the electrical energy is basically converted into mechanical energy of liquid motion through electrically induced change in the dielectric surface wettability [1]. Concept of electrowetting has been opted in electrostatic energy harvesting called Reverse-electrowetting in which mechanical energy is converted to electrical energy by the movement of conductive droplets against electrostatic force. *Fig.2* shows the mechanical to electrical energy conversion through reverse electrowetting.

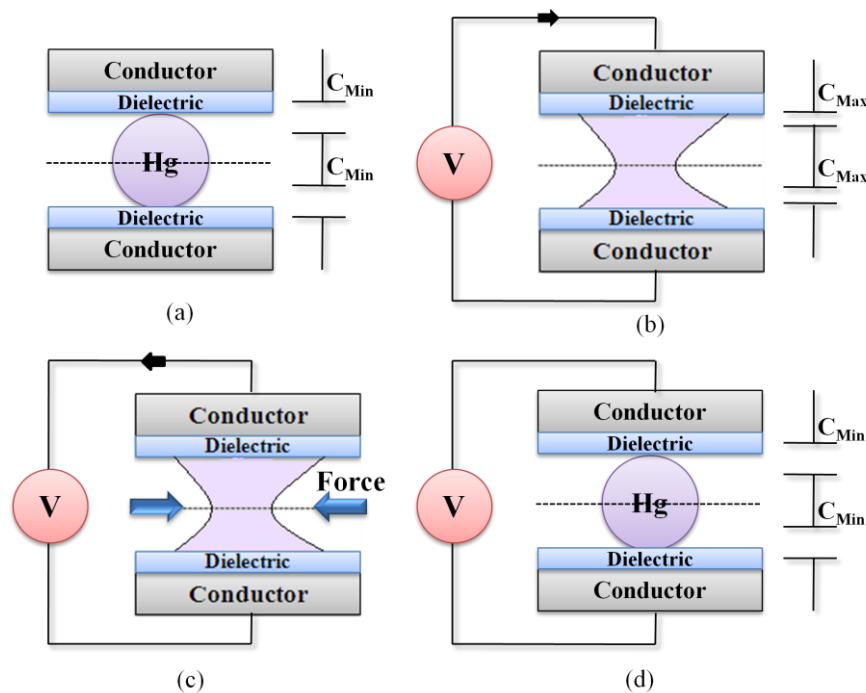


Fig.2. (a) A conductive droplet(Hg) in between two dielectric coated electrodes, (b) Applying biasing voltage for electrowetting, (C) Mechanical to electrical energy conversion, (d) Device reaches its initial position.

The fundamental device is nothing but a conductive fluid(Hg) in between two dielectric coated electrodes. Due to hydrophobic nature, the overlapping area between conductive fluid and dielectric coated electrodes is very less and therefore the device offers very small capacitance shown in *Fig.2(a)*. On applying voltage, the interfacial energy between conductive fluid and dielectric coated electrode decreases which leads to the spreading of fluid onto the solid. By this, the overlapping area increases results in increase in capacitance of the device as depicted in *Fig.2(b)*. Now to reduce the capacitance or overlapping area of the device, external force is applied against the electrostatic field, corresponding work done converted to electrical energy and flows back towards the voltage source as shown in *Fig.2(c)*. As the capacitance of the device reaches its minimum value, the device gets its initial position as depicted in *Fig.2(d)*. The same process will be continued for all vibration cycles.

For high energy harvesting, device capacitance should be very high [3]. This approach has a number of significant advantages over existing mechanical-energy-harvesting techniques

including very high power densities, up to $1\text{KW}/\text{m}^2$ and ability to directly utilize broad range of mechanical forces and displacements, including those not accessible by traditional piezoelectric, electromagnetic or electrostatic methods[1].

Chapter3

Device simulation

This energy harvester is nothing but a electrowetting based Microfluidic voltage variable capacitor. COMSOL Multi-physics fluid-flow module has been utilized to realize this device. The device is a hollow copper cylindrical structure which is coated with dielectric material on its inner surface. The lower half of the device filled with conductive fluid while the upper half of the device filled with dielectric fluid. Mercury and air have chosen as conductive and dielectric fluids respectively as shown in *Fig.3*. The contact angle and the interfacial tension between Mercury and air are 140° and 0.486N/m respectively.

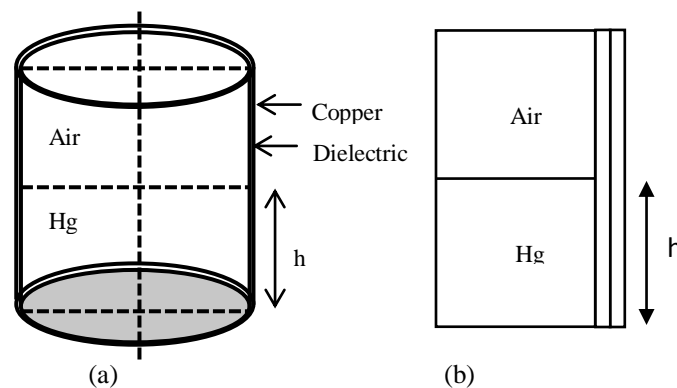


Fig.1 (a) Complete 3D model, (b) A 2D plane of the 3D model.

To reduce the computation time, instead of simulating complete cylindrical 3D structure, a 2D plane of the cylindrical structure has been simulated as depicted in *Fig.3*; the complete 3D structure will be just the replica of this plane only.

The device forms a cylindrical capacitor between the mercury and the copper body. At zero bias, the Hg-air contact angle is 140° which can be observed in *Fig.4* that's why the contact

length(h) between mercury and dielectric coated electrode is very small hence form a small capacitor.

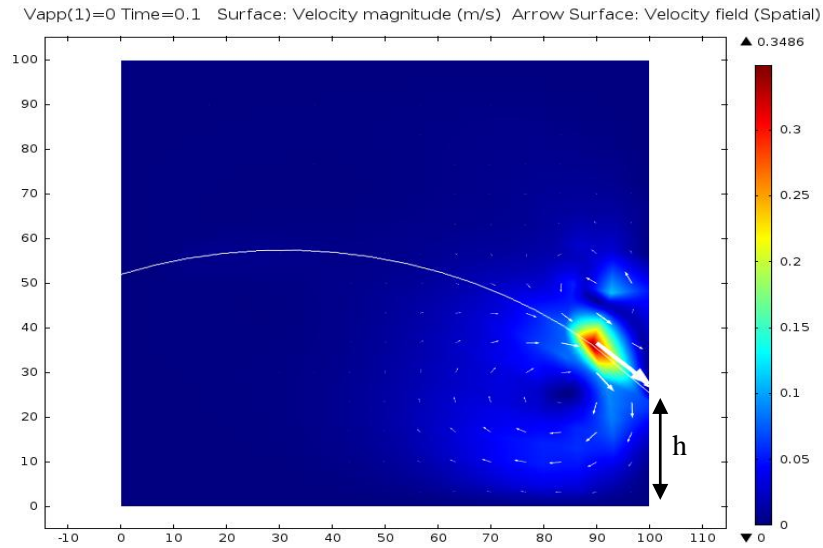


Fig.2.Contact length (h) between mercury and dielectric coated electrode at zero bias.

Capacitance of the device is given by,

Here,

$$C = \frac{2\pi\epsilon_0\epsilon_r h}{\ln(b/a)}$$

h = Contact length between Hg and dielectric coated electrode.

a = Inner radius of the cylinder.

b = Outer radius of the cylinder = a + d.

On applying external supply between copper body and mercury, the wettability of dielectric coating increases which leads to decrease in contact angle and increase in contact length(h) as shown in *Fig.5* thus, the capacitance of the devices increases. In *Fig.4* and *Fig.5*, the color legend shows the range of fluid velocity magnitude and arrow represents the direction of velocity field.

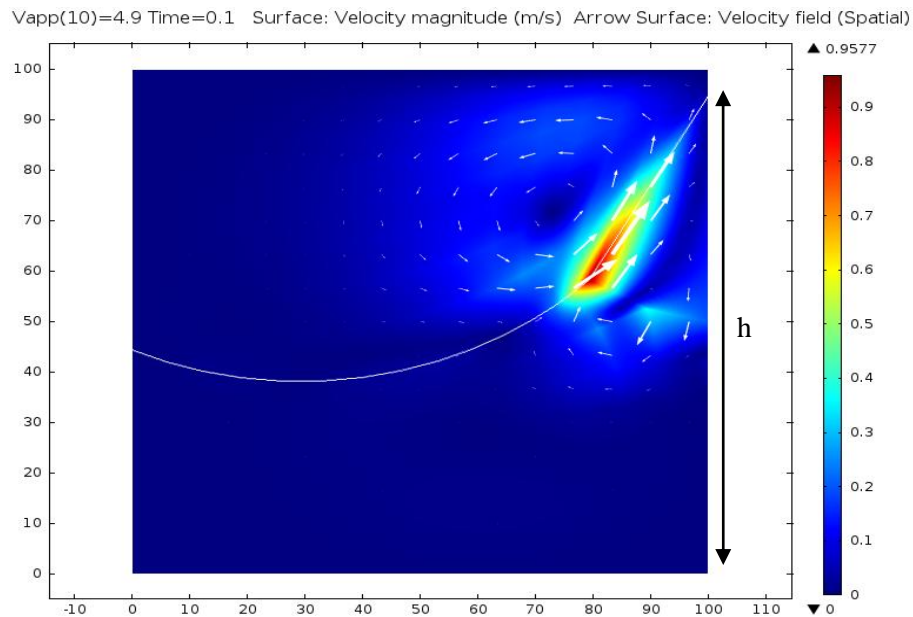


Fig.3.Contact length (h) between mercury and dielectric coated electrode at V=4.9Volt.

A Microfluidic device with high capacitance at low operating voltage is required for high energy harvesting. To achieve this objective all the parameters should be optimized. Dielectric material plays a key role in capacitance value. *Fig.6* shows the Capacitance variation of the device Vs applied voltage for various dielectric materials, keeping radius of device=1 μ m and dielectric thickness=100nm. We can observe that with the increase in dielectric constant all C_{Max} , C_{Min} and ΔC are increased. Also operating voltage also significantly reduced. From the plot, it is clearly clear that on using High-K dielectric material, the device will have higher capacitance with lower operating voltage. Onwards we will consider Titanium dioxide (TiO_2) as dielectric material for all other parameter optimization.

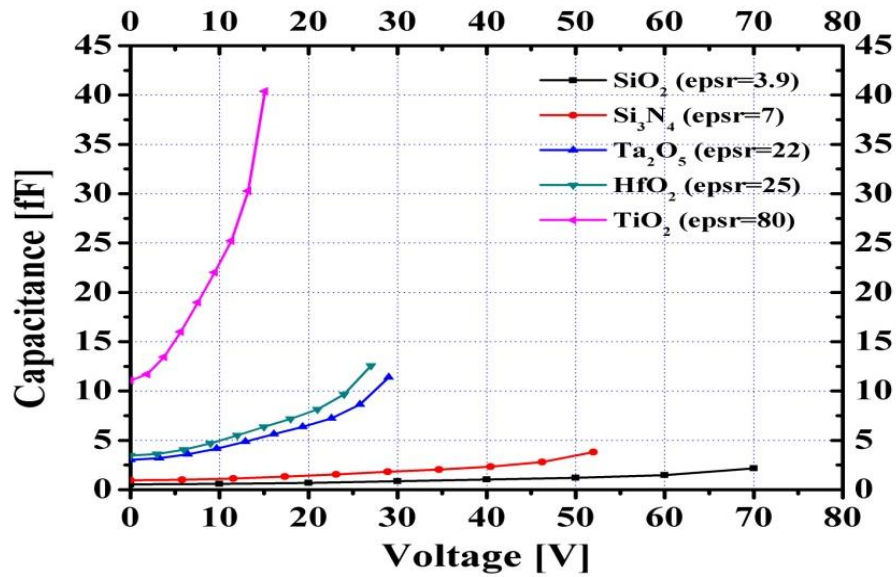


Fig.4.Capacitance Vs Voltage for various dielectric materials[4].

Dielectric thickness also plays big role variation in capacitance. *Figure 7* shows the Capacitance variation Vs applied voltage for various dielectric thickness (keeping dielectric constant=80 and radius of device=1 μ m) and observed that decreasing the thickness of dielectric material, one can further increase the capacitance and decrease the operating voltage requirement.

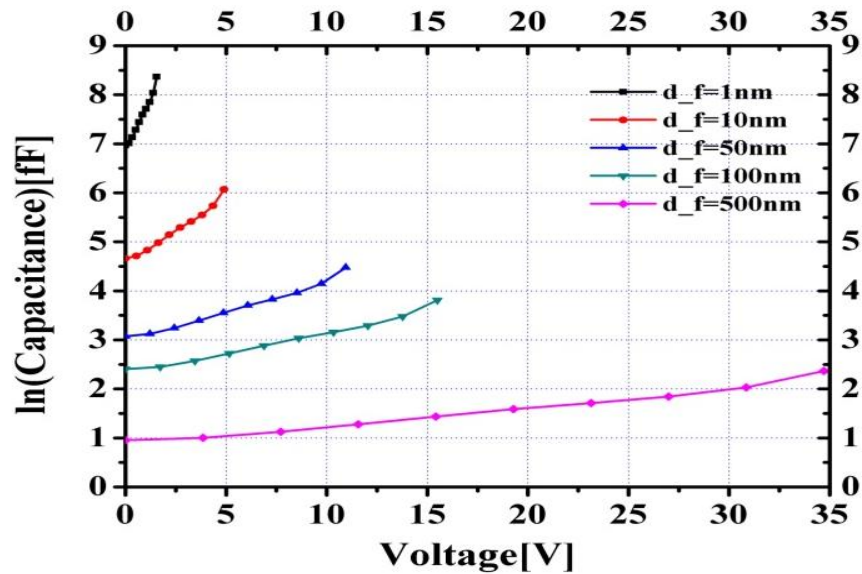


Fig.5.Capacitance Vs Voltage for various dielectric thicknesses.

At 1nm TiO₂ thickness, very high capacitance of value 4.302pF at very small operating voltage of 1.55V has been achieved but it is very difficult to deposit 1nm uniform thick vertical dielectric that's why 10nm dielectric thickness has been preferred for which maximum capacitance is 0.431pF at an operating voltage of 4.9V.

After having insight of dielectric and thickness of dielectric it will be interesting to see the effect of radius of cylinder on capacitance variation as well as operating voltage. From fig.8 it is evident that with increase the radius, increase in capacitance but the operating voltage independent.

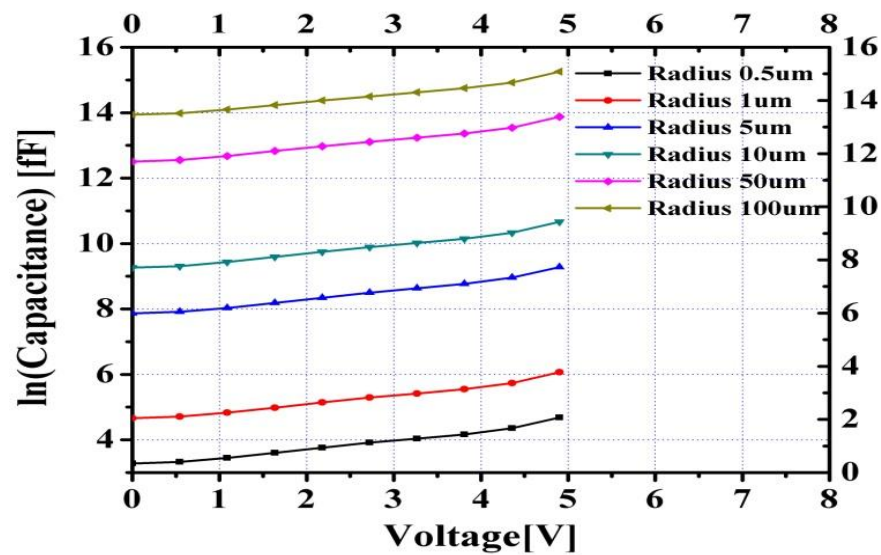


Fig.6.Capacitance Vs applied voltage for various radius of cylinder.

Table1. Capacitances for various radius of cylinder.

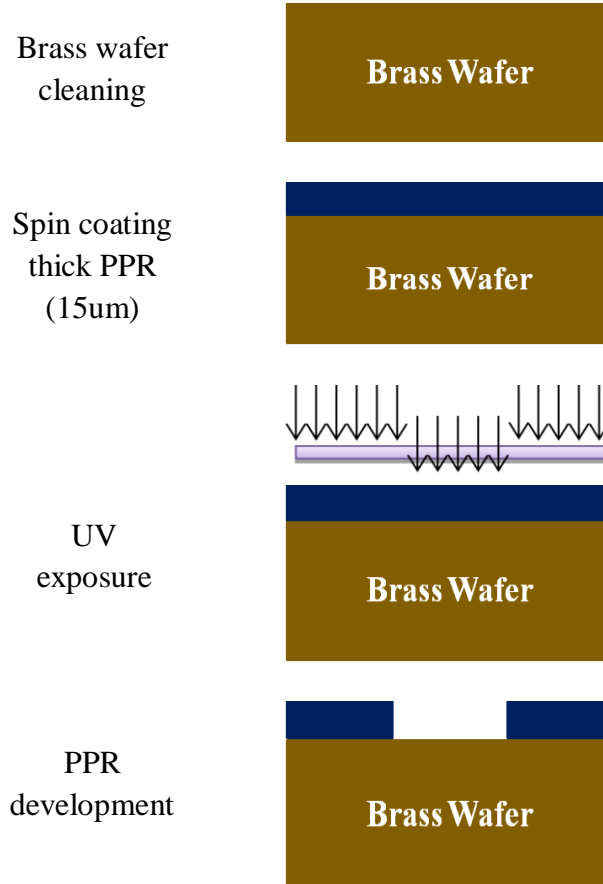
Radius of cylinder [μm]	C _{Max} [fF]	C _{Min} [fF]	ΔC [fF]	V _{Max} [V]
0.5	108.38	26.58	81.8	4.9
1	431.44	106.014	325.45	4.9
5	10740.03	2607.46	8132.57	4.9
10	42968.64	10535.72	32432.92	4.9
50	1061333.56	270045.55	791288.01	4.9
100	4213696.71	1132321.28	3081375.43	4.9

From the table 1, it can be concluded that instead of using single big droplet if one use multiple small droplets of same volume then the total capacitance will be much more and hence the harvested energy. The reason behind this is area to volume ratio is much high in case of multiple small droplets as compare to single big droplet of same volume. Use of multiple conductive droplets introduces the need of immiscible dielectric droplets which need to be placed in between the conductive droplets. Polydimethylsiloxane (PDMS) is a good choice for dielectric fluid. Dielectric fluid doesn't participate in the actual operation of the device; it just used to provide isolation between the conductive droplets therefore the volume occupied by these dielectric droplets reduces the capacitance per unit volume offered by the device. In spite of this also, it is highly recommended to use multiple small droplets for high energy harvesting.

Chapter4

Device fabrication using Deep X-ray Lithography

4.1 X-ray mask fabrication:



Ni+Gold
electroplating (15um)



Dissolving PPR



Poly-amide spin
coating



SS ring Bonding



Brass wafer etching



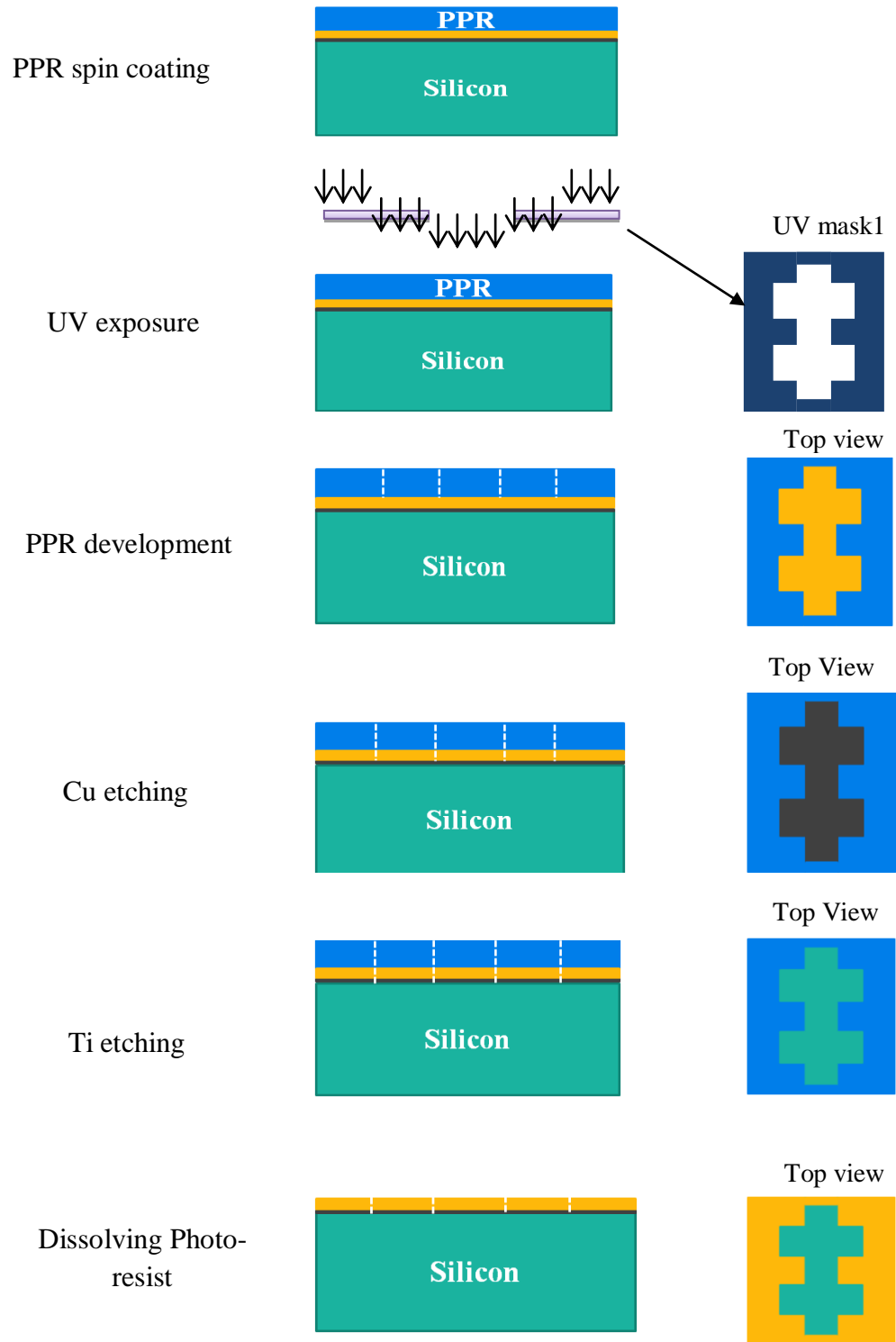
4.2 Process flow of Reverse-electrowetting based energy harvester:

Standard Si cleaning

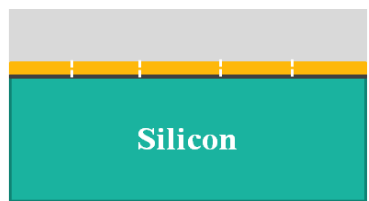


Ti + Cu deposition
(50nm+200nm)

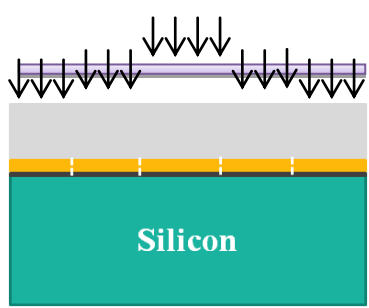




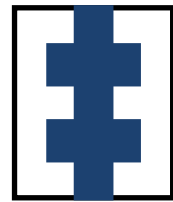
PMMA bonding



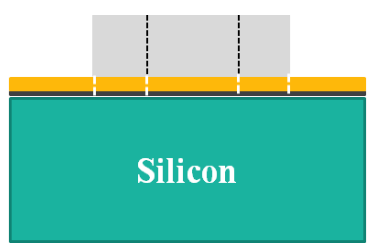
X-ray exposure



X-ray mask



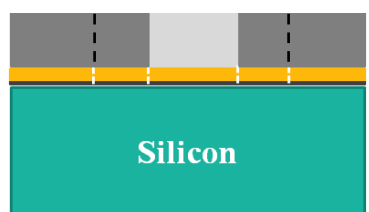
PMMA development



Top view



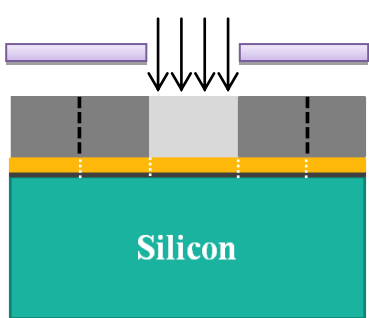
Ni electroplating



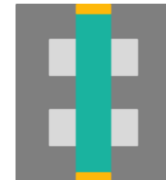
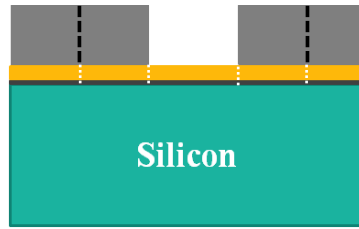
Top view



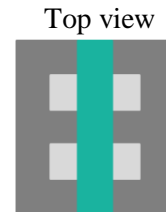
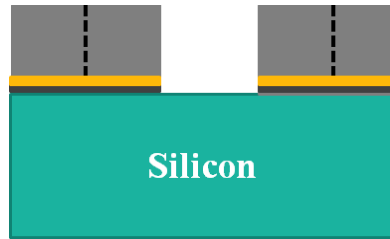
X-ray exposure



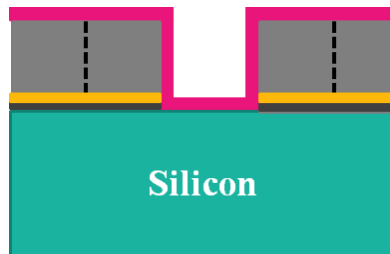
PMMA
development



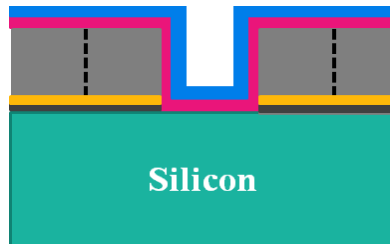
Cu + Ti contact
line etching



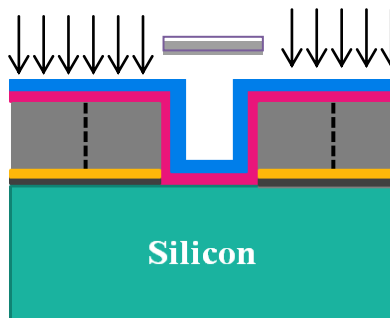
Dielectric layer
deposition
(200nm)

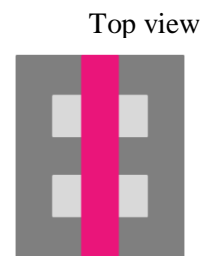
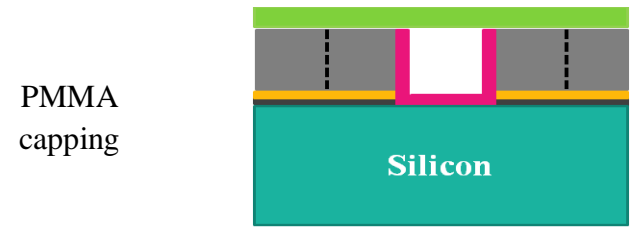
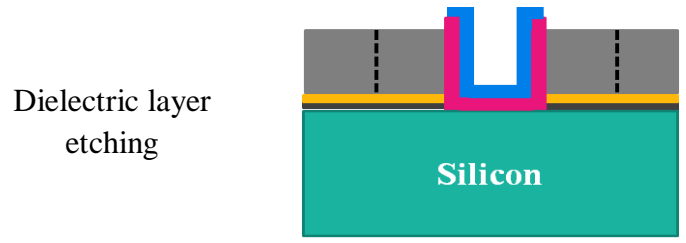
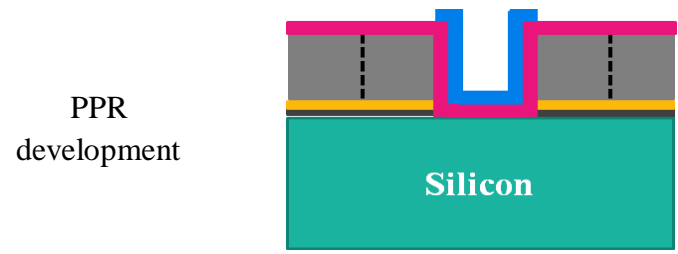


Spin coating
PPR



UV exposure

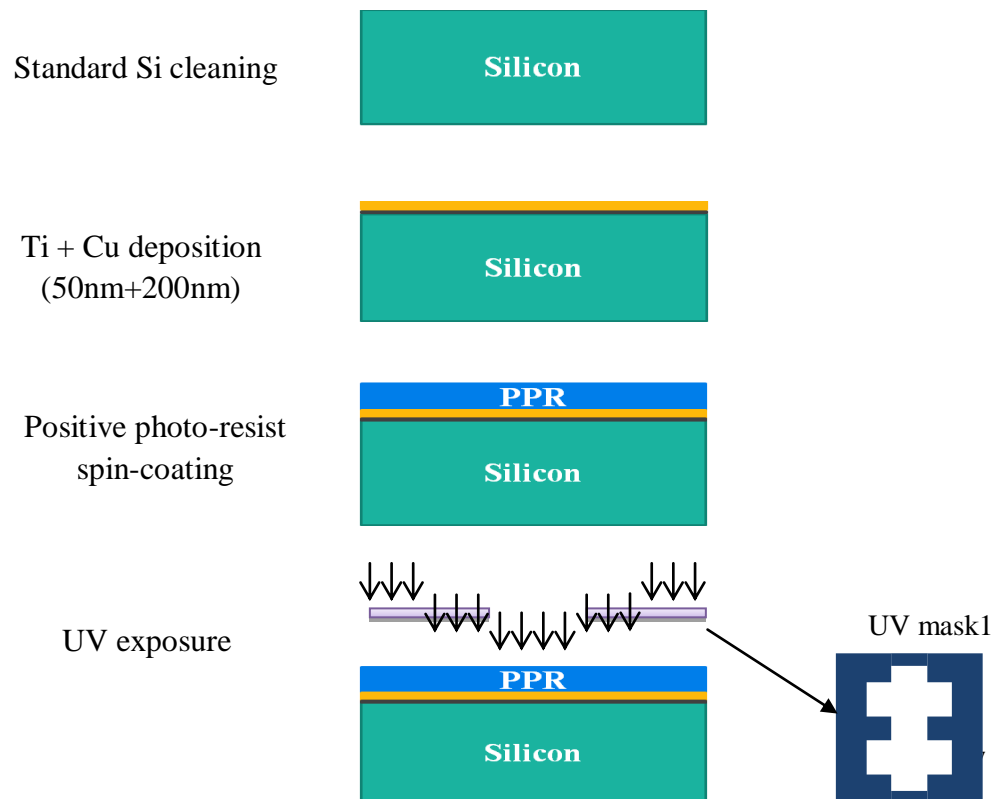




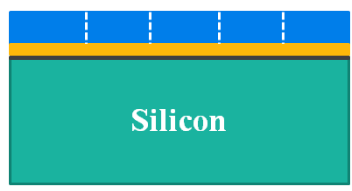
Chapter5

Device fabrication using UV lithography with Positive photoresist

5.1 Process flow of Reverse-electrowetting based energy harvester:



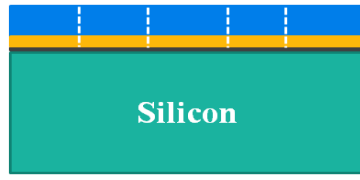
PPR development



Top view



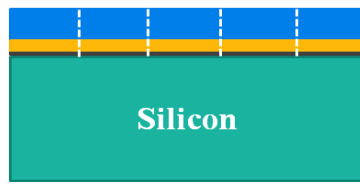
Cu etching



Top View



Ti etching



Top View



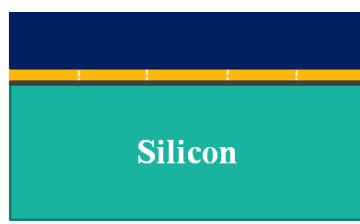
Dissolving Photo-resist



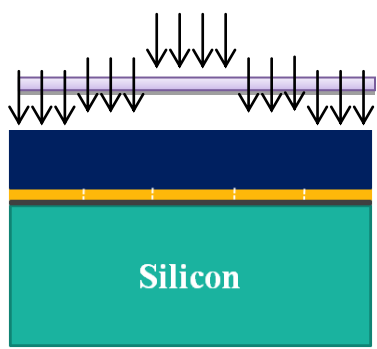
Top view



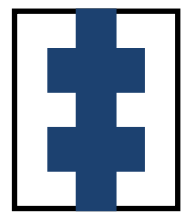
Spin coating thick PPR (25um)



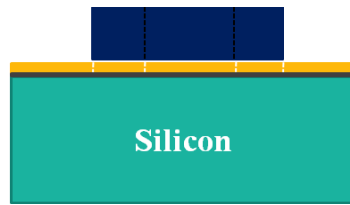
UV exposure



UV MASK2



Thick PPR development



Top view



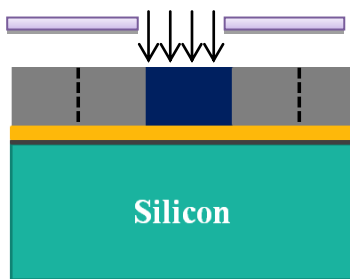
Nickel electroplating (25um)



Top view

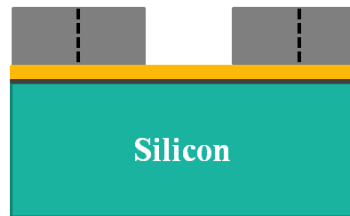


UV exposure



UV MASK3

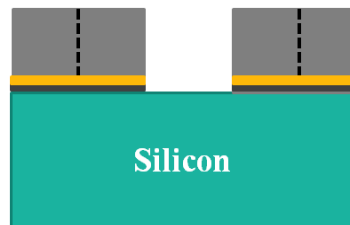
PPR development



Top view



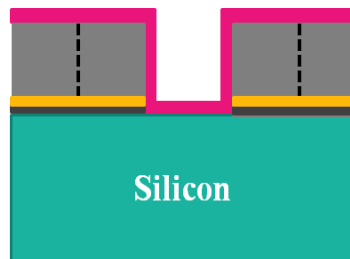
Cu + Ti contact line etching



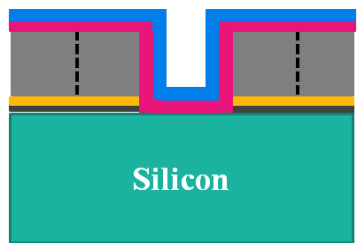
Top view



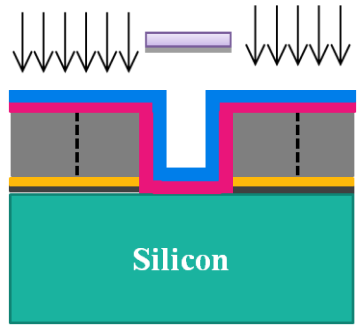
Dielectric layer deposition (200nm)



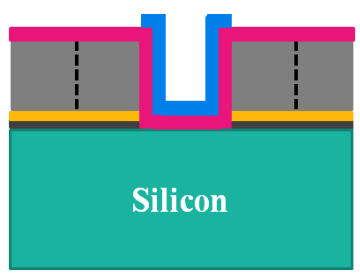
Spin coating PPR



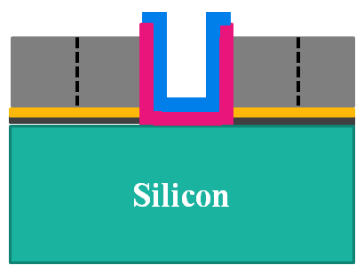
UV exposure



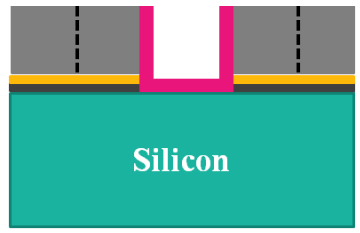
PPR development



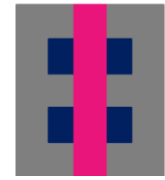
Dielectric layer etching



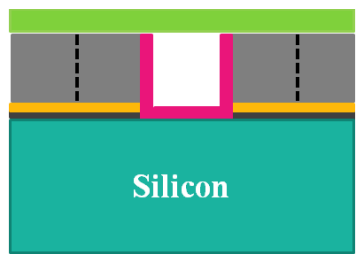
Dissolving PPR



Top view



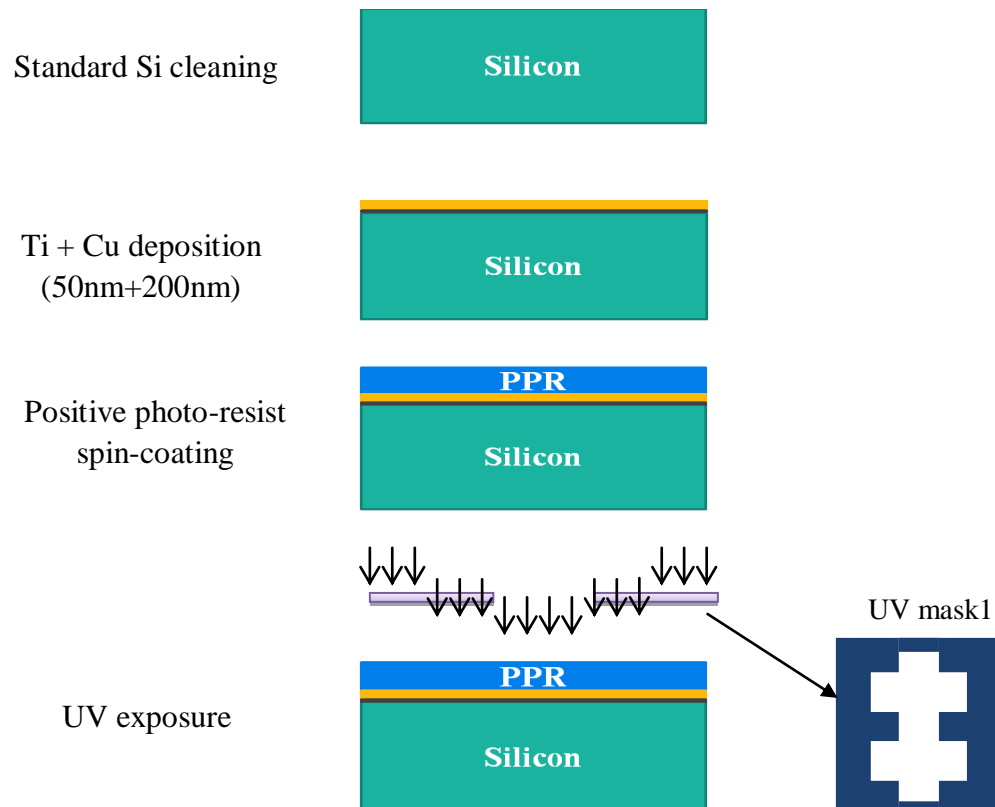
PMMA capping



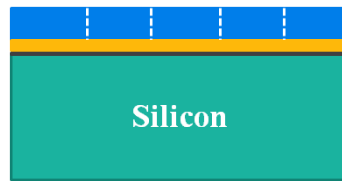
Chapter6

Device fabrication using UV lithography with SU-8

6.1: Process flow of Reverse-electrowetting based energy harvester



PPR development



Top View



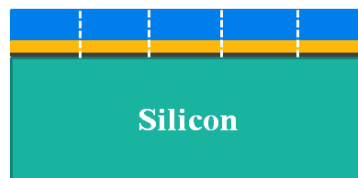
Cu etching



Top view



Ti etching



Top View



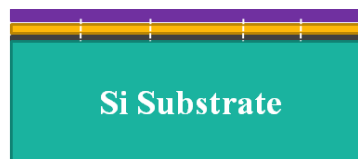
Dissolving Photo-resist



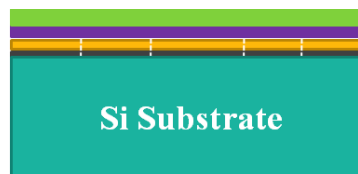
Top view

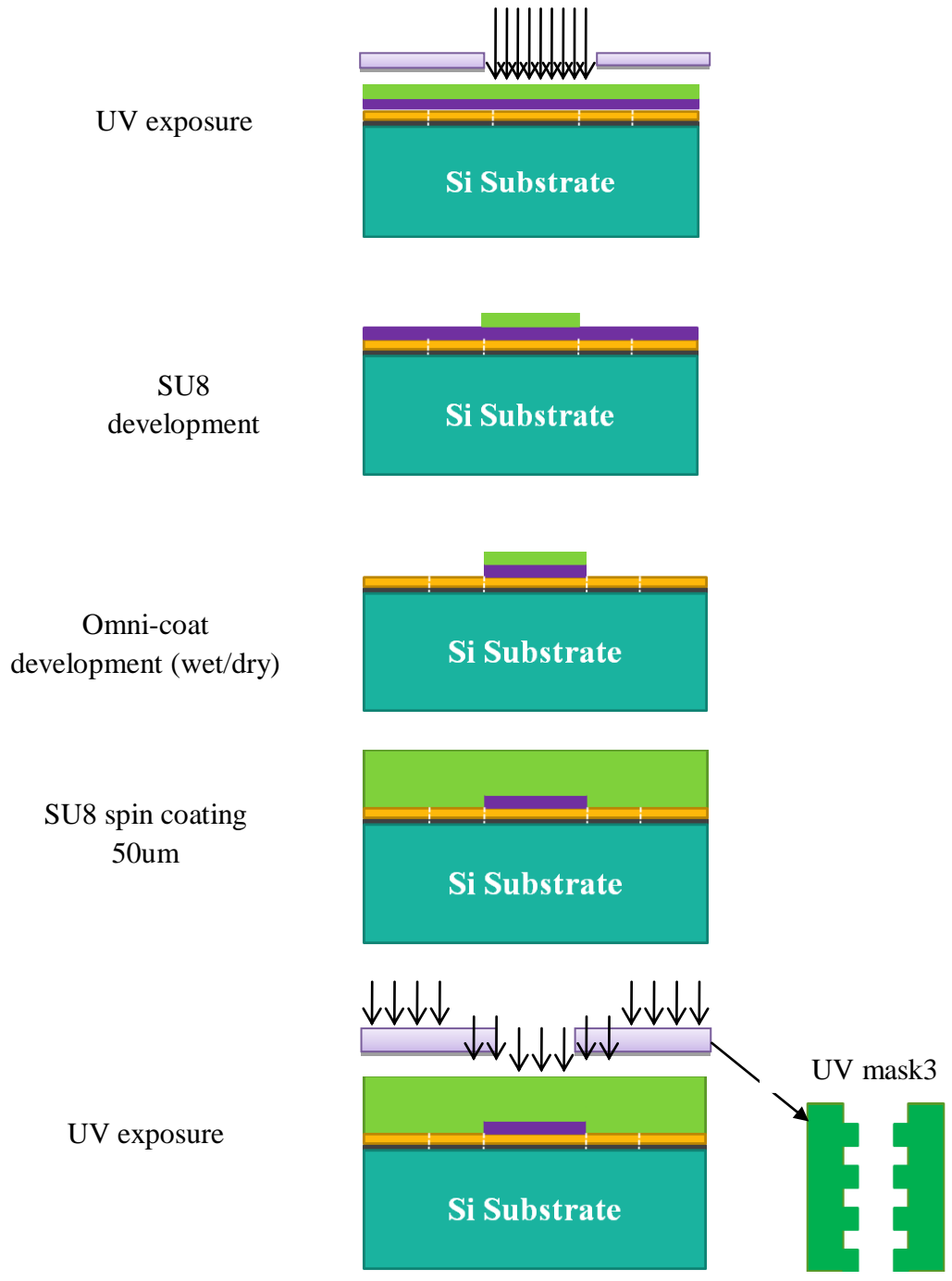


Omni-coat

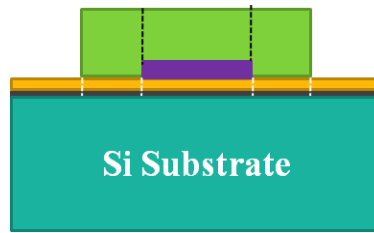


Su8 spin coating
1-2um





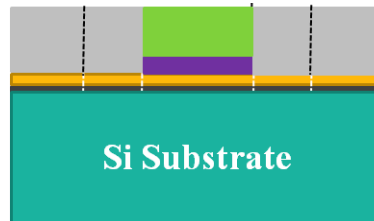
SU8 development



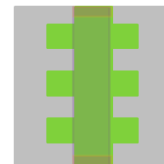
Top view



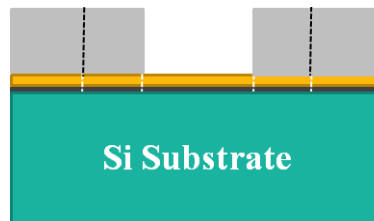
Ni electroplating



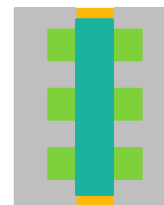
Top view



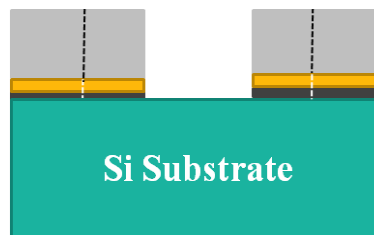
PG removal



Top view



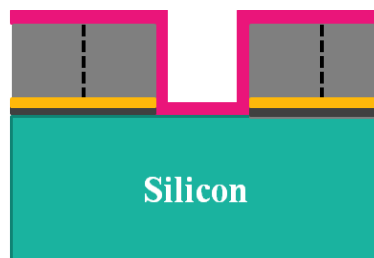
Cu + Ti contact
line etching



Top view

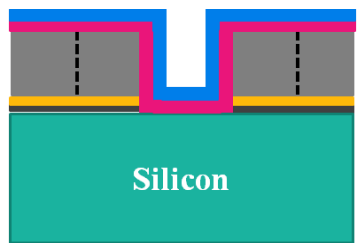


Dielectric layer
deposition (100nm)

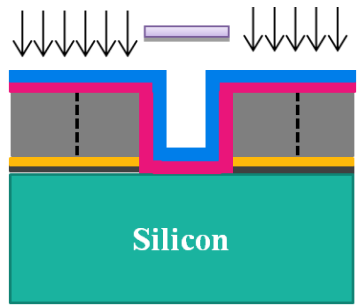


Silicon

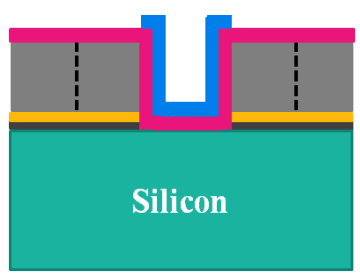
Spin coating PPR



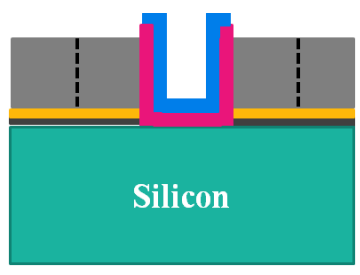
UV exposure



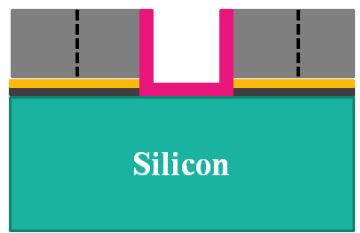
PPR development



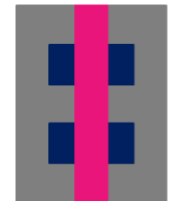
Dielectric layer etching



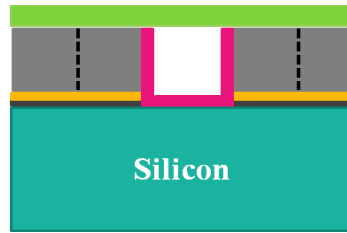
Dissolving PPR



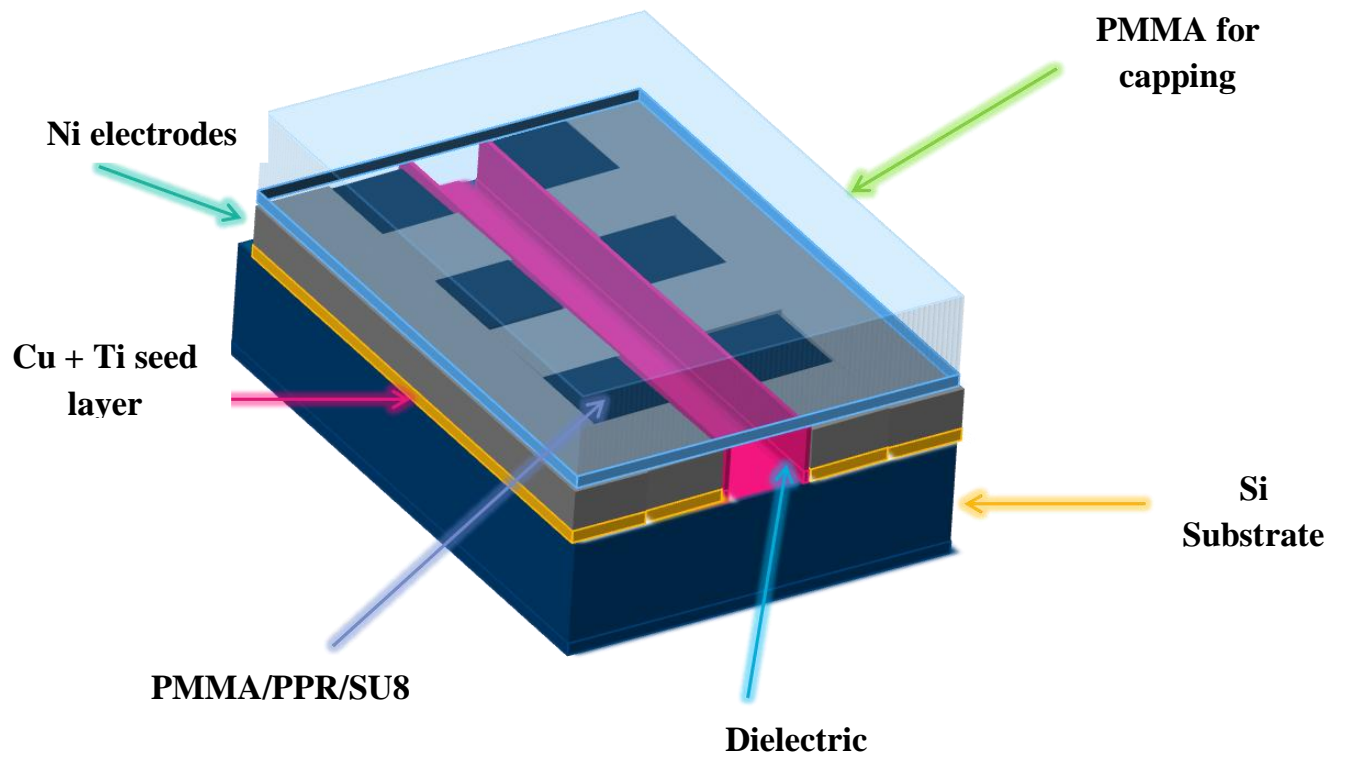
Top view



PMMA capping



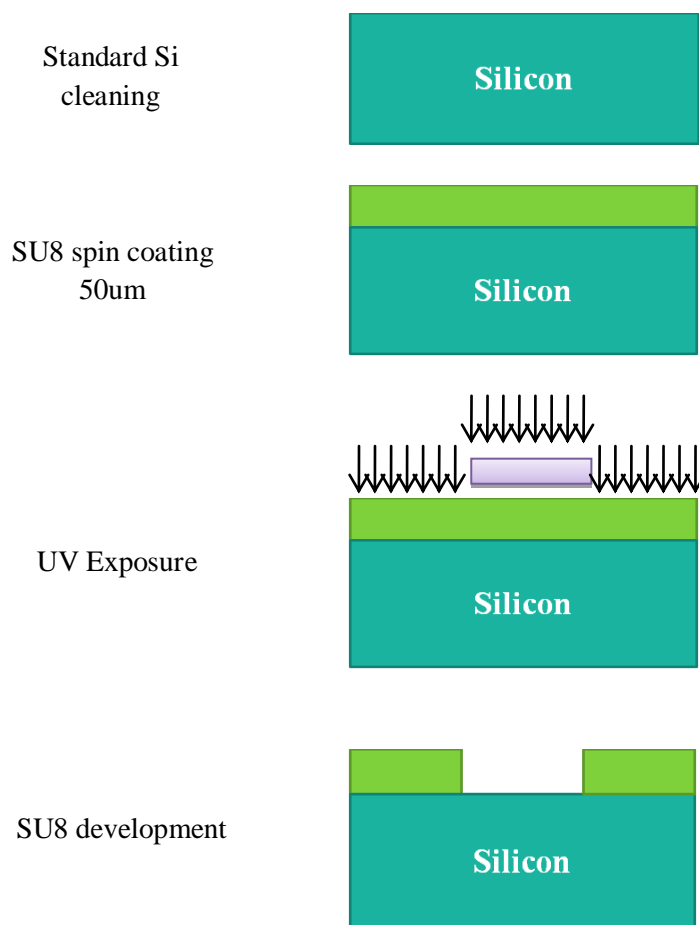
6.2: Isometric view of the energy harvester:



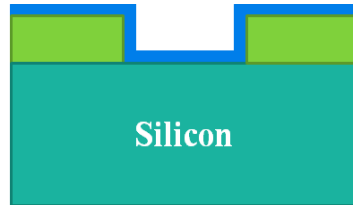
Chapter7

Device fabrication without electroplating

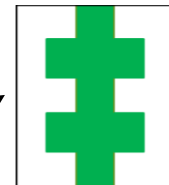
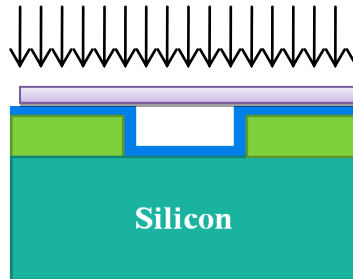
7.1: Process flow of Reverse-electrowetting based energy harvester:



Positive Photo-resist
spin-coating

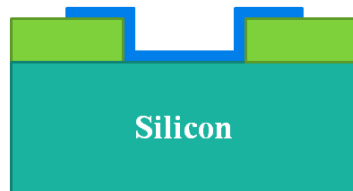


UV exposure

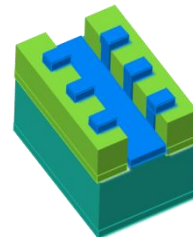


UV mask

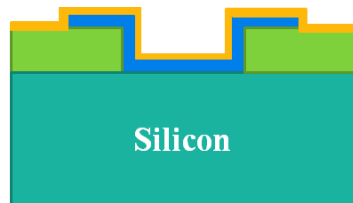
Positive Photoresist
development



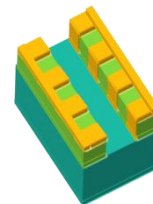
3D View



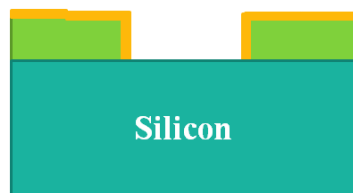
Cu deposition
200nm



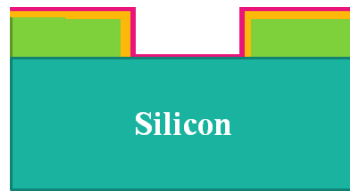
3D View



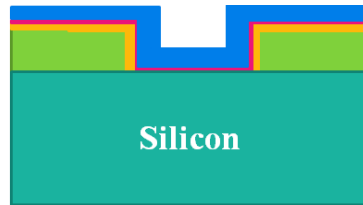
Lift off



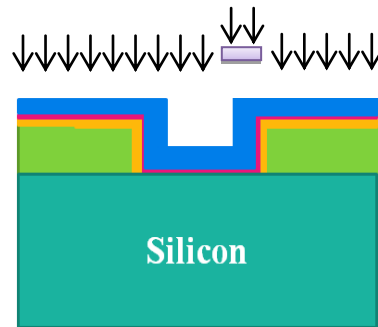
Dielectric deposition
100nm



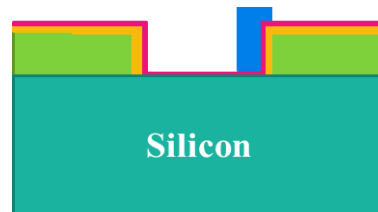
PPR spin coating



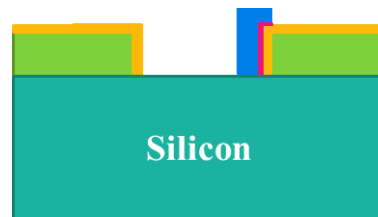
UV exposure

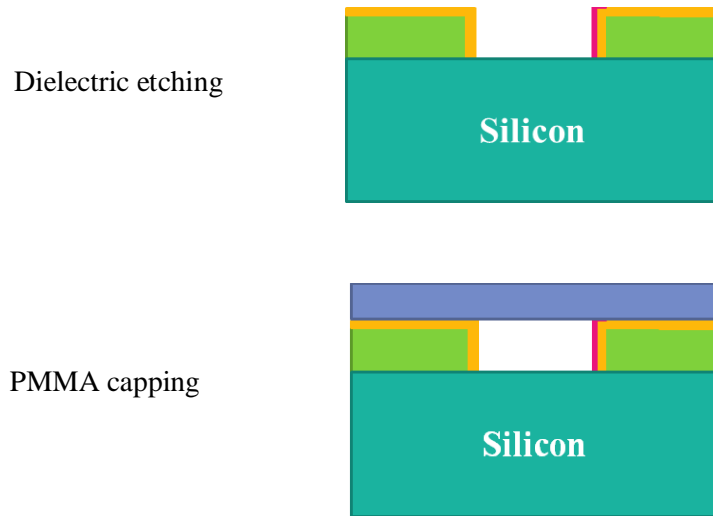


PPR development

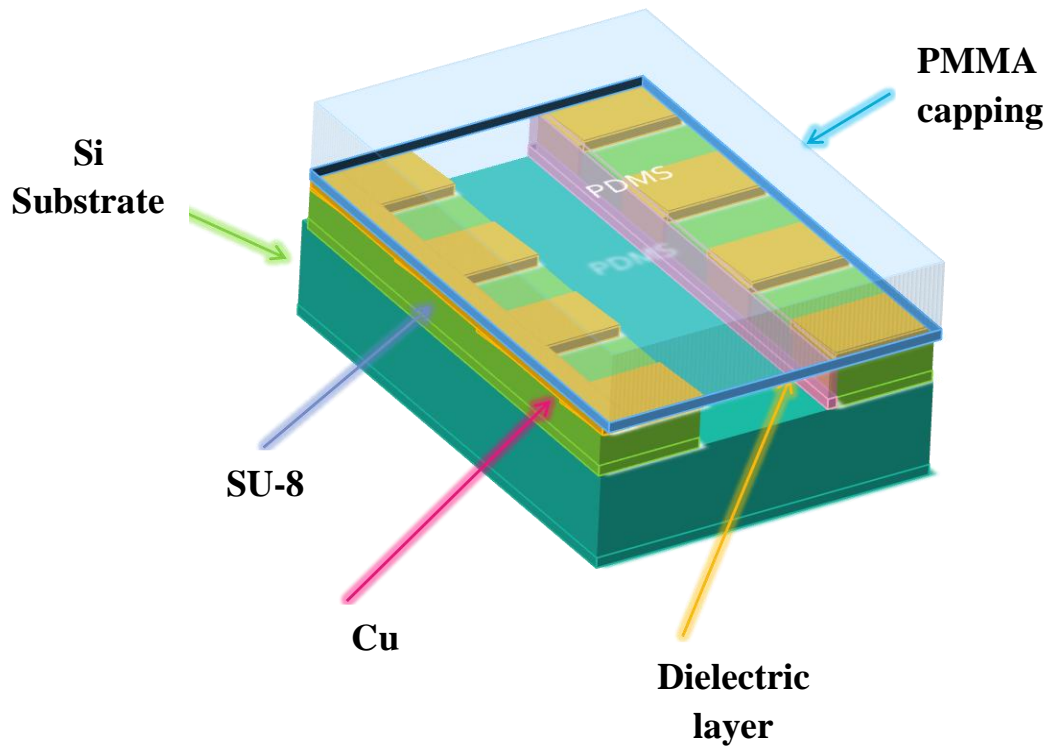


Dielectric etching





7.2: Isometric view of the energy harvester:



Chapter8

Implementation

8.1 Device fabrication using deep X-ray lithography:

8.1.1 X-ray masks fabrication: For X-ray absorption, there is constraint between the selection of masking material and its thickness. High-Z materials require less thickness and low-Z materials require high thickness for the absorption of X-rays. For X-ray Lithography, we have used 3-10KeV photon energy range in Indus BL-07. For this range, 15um Gold has very low transmittance means very high absorbance as depicted in Fig1.

Au Density=19.3 Thickness=15. microns

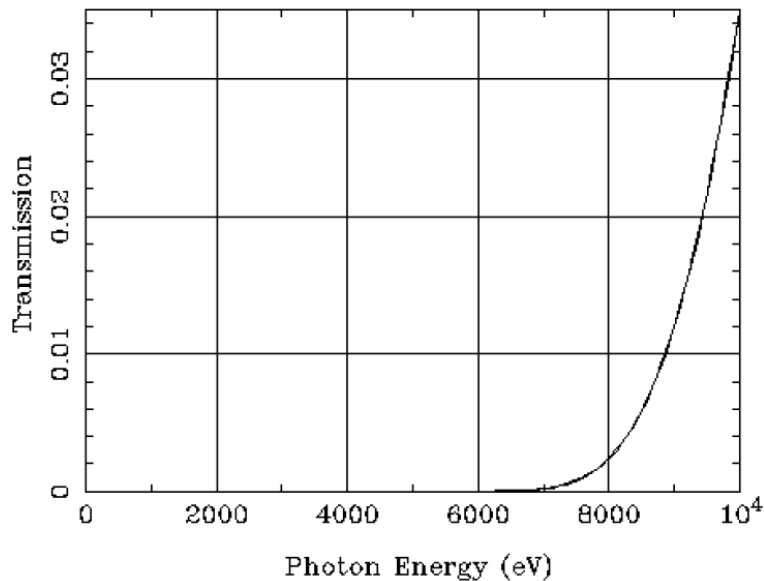


Fig1. Transmittance Vs Photon energy for 15um thick Gold.

Hence we have chosen 15um gold for X-ray mask. Two X-ray masks have been utilized in the first process flow. For fabricating these masks, two 4'' brass wafers have been taken. We cleaned these brass wafers with Acetone, IPA and DI-water. We spin coated Positive photo-resist (AZ4903) on the brass wafers with the spin rate of 500RPM for 8secs then 1400RPM for 60secs at the acceleration of 500RPM^2 which gives 15um thickness then we put the wafers onto the hot plate at 100°C for 5min then wait till it acquire room temperature. UV exposure has been performed onto the wafers with mask1 and mask2 as shown in below figures for 400secs which provide the required dose of $720\text{mJ}/\text{cm}^2$. After this we develop the photo-resist for 5mins in AZ400K developer (1:3) and dried the wafers with N_2 .

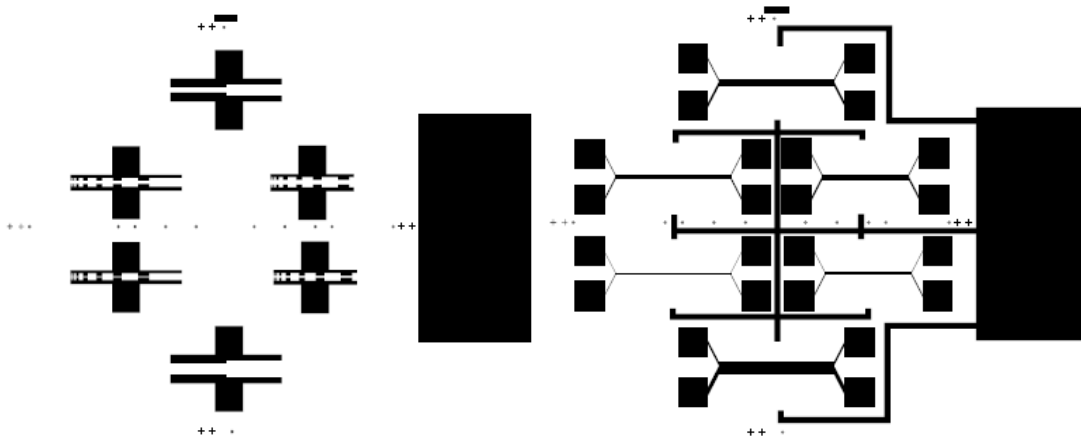


Fig2. Gelatin mask1 & mask2 for making X-ray masks.

Now sample is ready for gold electroplating. The area where electroplating has to be done is approximately 0.6dm^2 for both the samples. To provide good adhesion between brass wafer and gold a seed layer of Nickel has been electroplated first. Nickel electroplating has been done at a current density of $3\text{A}/\text{dm}^2$ at 65°C for 3mins which provides a thickness of 1-2um then we put the sample in gold electroplating system in which electroplating has been carried out at a current density of $0.15\text{A}/\text{dm}^2$ at 50°C for 80mins. The achieved thickness is 15um as desired. After this we dissolve the Positive Photo-resist in acetone and dried with N_2 . Fig3 shows the electroplated samples after dissolving Positive photo-resist.

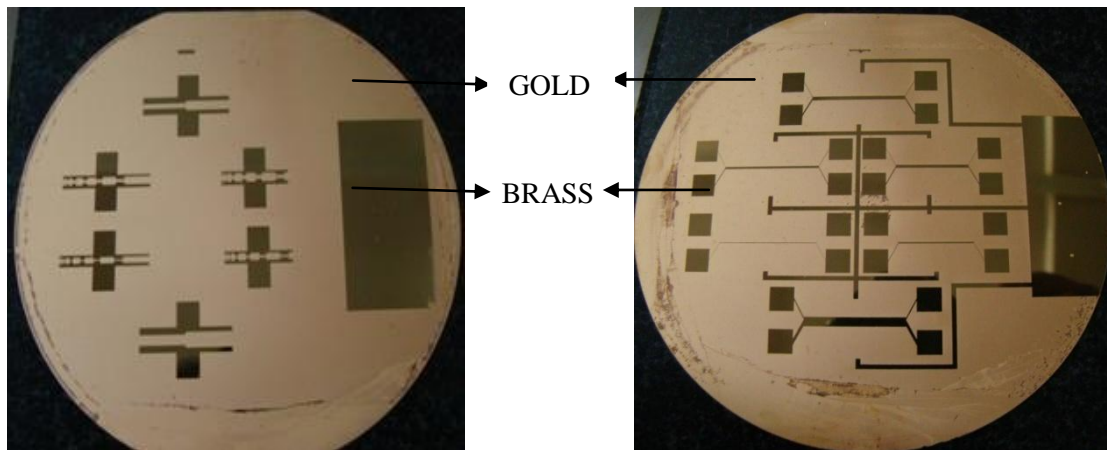


Fig3. Gold electroplated brass wafers after dissolving PPR.

Onto these two samples we have spin coated poly-amide at a spin rate of 500RPM for 45secs with a ramp-up and ramp-down of 5secs then we put these samples on hot plate for gradual heating from room temperature to 310°C as depicted in the fig4.

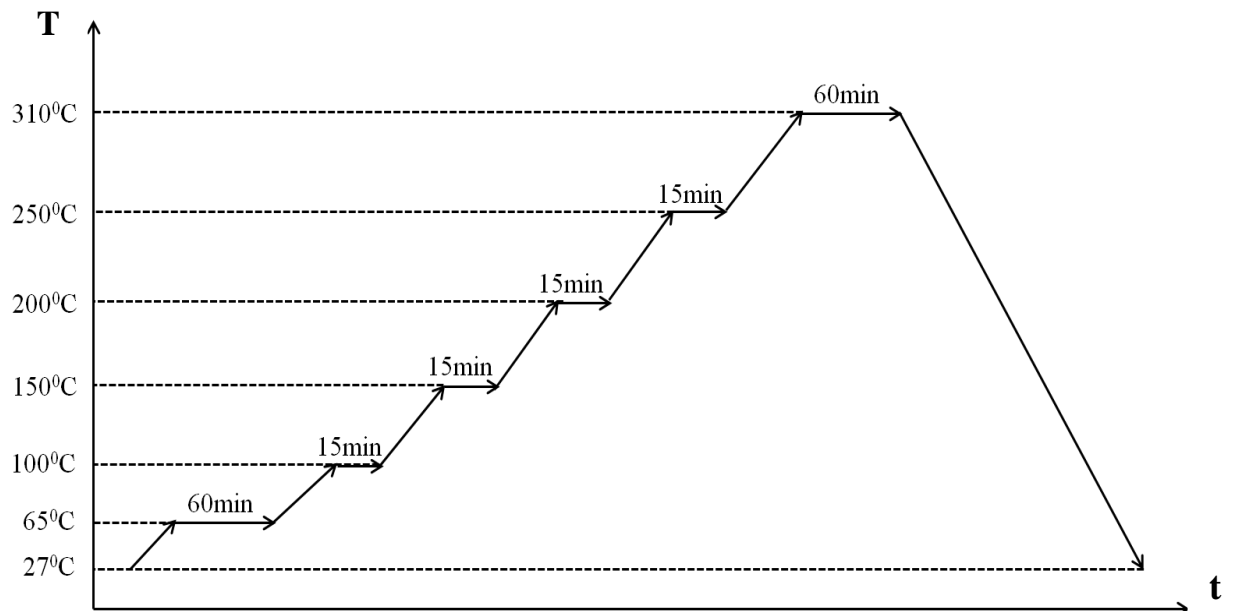


Fig4. Gradual heating on Polyimide coated sample.

To fit the X-ray mask properly onto the mask holder we need to bond stainless steel ring. Before bonding we have cleaned the SS rings by putting it into HNO₃ solution for 20mins. We have used JB WELD paste for the bonding. After pasting SS ring onto the samples we applied weights for 12Hrs.

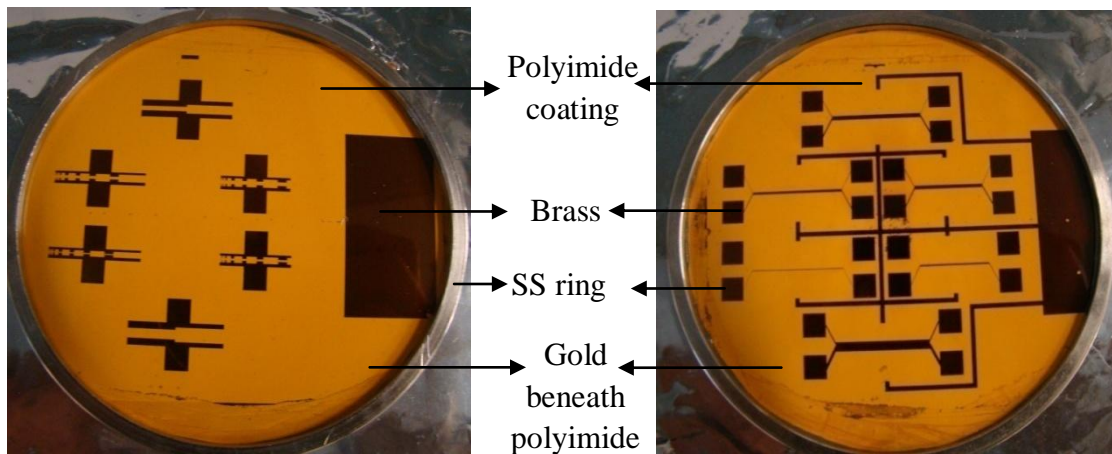


Fig5. Polyimide coated sample and bonded SS ring to support the polyimide membrane after etching

Now the final task is to etch brass wafer. For doing this etching we have used Concentrated HNO_3 which was diluted in de-ionized water with 3:2 ratio. The complete etching took round 20mins after that we rinse the mask with DI-water and dried it. Figure 6 shows the X-ray masks made for energy harvester fabrication.

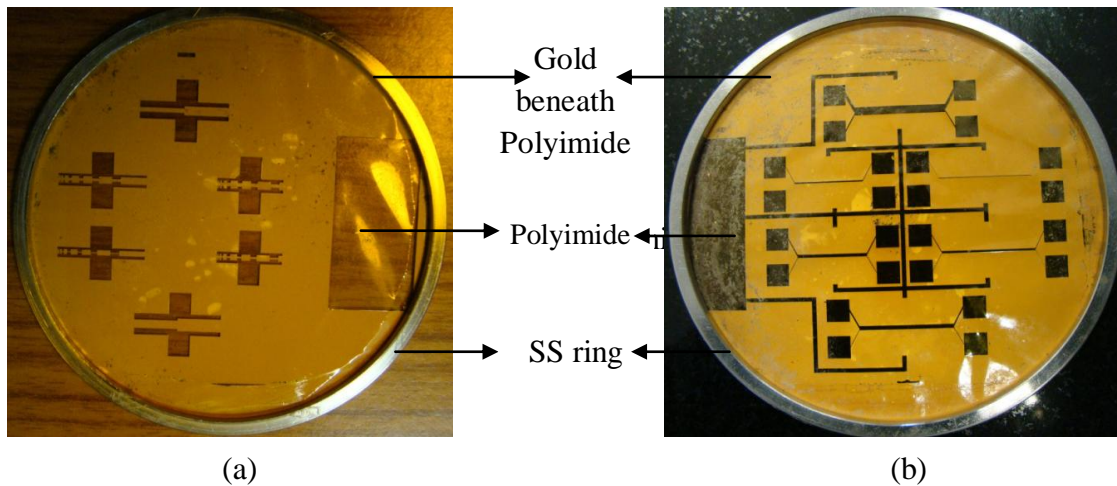


Fig6. X-ray Masks (a) Mask1, (b) Mask2.

8.1.2 Reverse-electrowetting based energy harvester fabrication

Firstly Si wafer has been taken for standard RCA (RCA1: $\text{NH}_4\text{OH}:\text{H}_2\text{O}_2:\text{H}_2\text{O}=1:1:5$ at 80°C for 10mins; RCA2: $\text{HCL}:\text{H}_2\text{O}_2:\text{H}_2\text{O}=1:1:5$ at 80°C for 10mins) and Piranha cleaning ($\text{H}_2\text{SO}_4:\text{H}_2\text{O}_2 = 1:1$ for 10mins). After drying the wafer with N_2 , we sputter Ti and Cu of 50nm and 200nm respectively. Ti layer acts as a diffusion barrier for Cu and also improves Cu adhesion with Si. We spin coated PPR (AZ5214E) onto the wafer with the spin rate of 500rpm for 8secs and then 2000rpm for 45secs with the acceleration of 500rpm^2 which has given a thickness of $\sim 2\mu\text{m}$. To evaporate the solvent from the PPR, we prebake it at 100°C for 60secs. Now the sample is UV exposed at the UV intensity of $1.7\text{mW}/\text{cm}^2$ for 20secs with the UV mask1 as shown in below fig7.

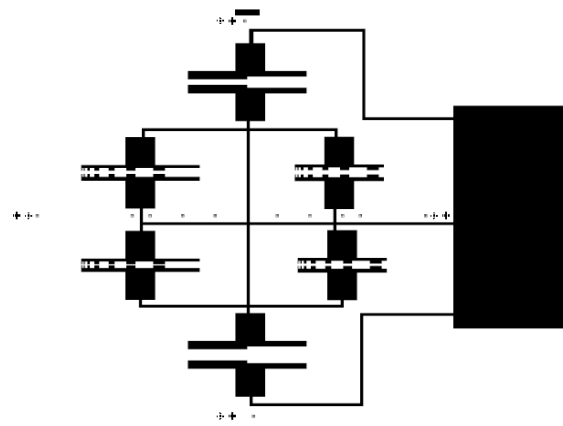


Fig7. UV Mask1

We put the exposed sample in AZ726 MIF developer for 30secs then we rinsed the sample with DI water and dried with N_2 . Cu and Ti are now etched by Ammonium peroxydisulphate ($\text{APS}=37\text{g} + 80\text{ml water}$) at 40°C and $\text{HF}:\text{H}_2\text{O}_2:\text{H}_2\text{O}=1:1:20$ at room temperature respectively. After this we cleaned the sample with DI water and dried with N_2 . Fig8 shows the images of all the steps.

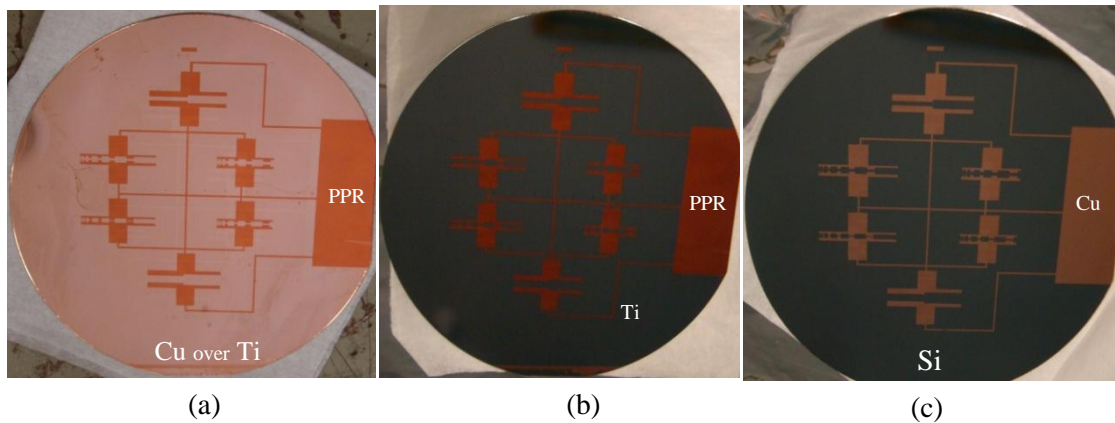


Fig8. (a) PPR patterns on Ti + Cu coated Si substrate, (b) Sample after Cu etching, (c) Sample after Ti etching

The next step is to bond PMMA sheet of 200um with this sample. For this bonding we have used Cyno-acrylate. After removing sticker from the PMMA sheet, we paste the sheet with the sample by the Cyno-acrylate then we put weight onto the sample for 1Hr in order to get good bonding strength then we left the sample for 24Hrs for drying. After drying, we remove the other sided sticker and put the sample for curing at 85°C for 7.5Hrs. Fig9 shows the cured PMMA bonded sample.

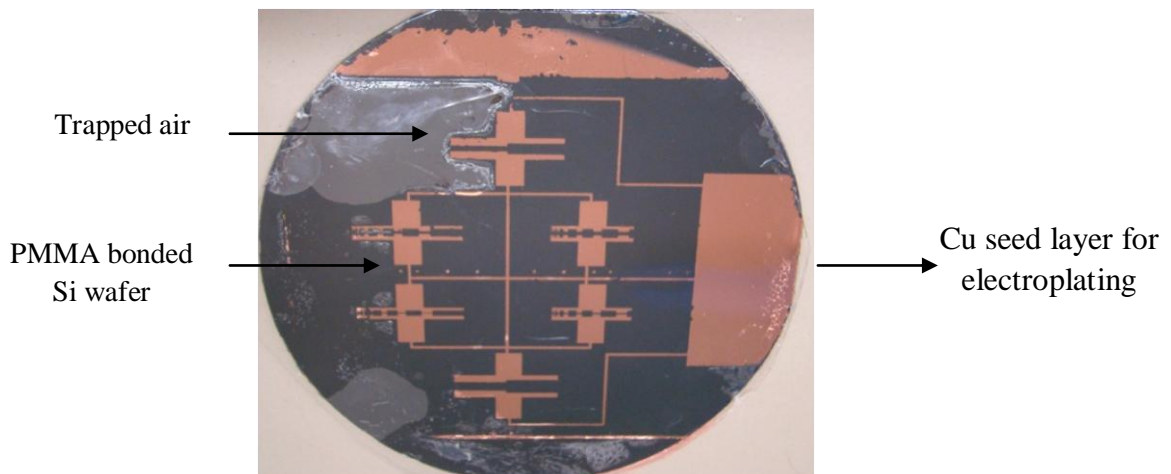


Fig9. PMMA bonded sample.

Now the sample is ready for X-ray exposure. Firstly we aligned the X-ray mask according to the sample by microscope then fitted both sample and mask to the mounting stage with the help of Iron ring. Below fig10 shows the complete assembly.

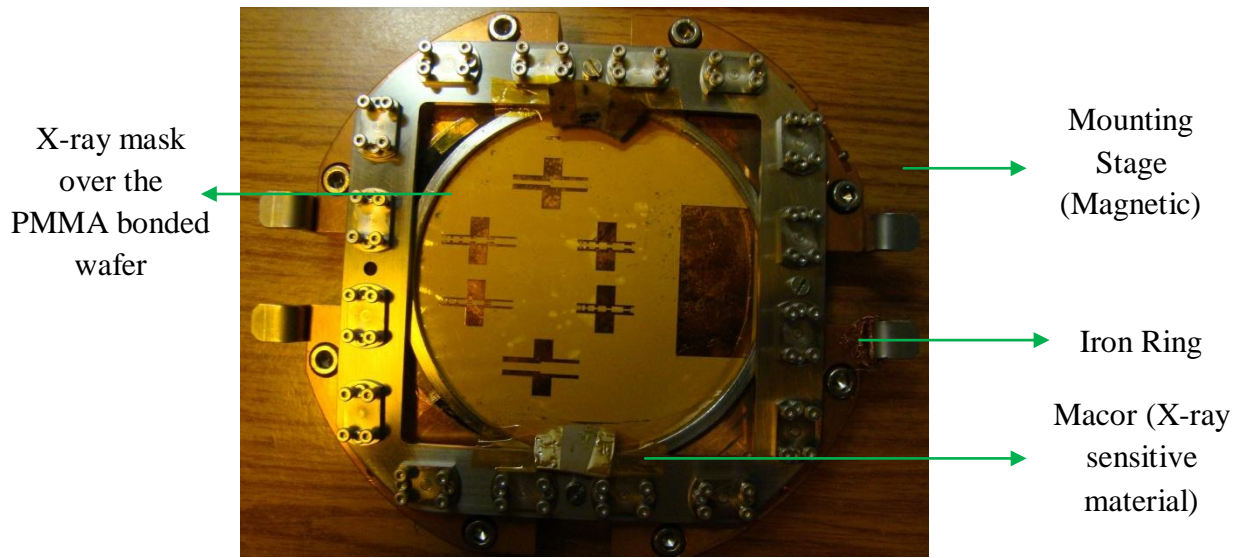


Fig10. Complete assembly of sample and mask holder.

The holder assembly is then fitted inside the Lithography machine. For 200um thick PMMA, required dose is 90000mAsec.

$$\text{Dose} = \text{Number of scan} * \text{Average current} * \text{time}$$

$$\text{Dose} = \text{Number of scan} * (I_{\text{Initial}} + I_{\text{Final}})/2 * (\text{Beam length}/\text{Scan speed})$$

Here,

$$\text{Beam length} = 12\text{mm}$$

$$\text{Scan speed} = 30\text{mm/sec}$$

Rests of the parameters vary with time.

Fig11 (a) shows the sample after exposure. We can observe that X-rays exposed portion has different color as compare to unexposed portion. After exposure we put the sample in GG developer (Di-ethylene glycol butyl ether: Morpholine: 2-amino ethanol: DI water: 12: 4: 1: 3) for 14 hrs. Further we put the sample in PMMA Rinser (Diethylene glycol butyl ether: DI water: 4:1) for 15mins then we rinsed the sample with DI water and dried with N₂. Fig11 (b) shows the sample after development.

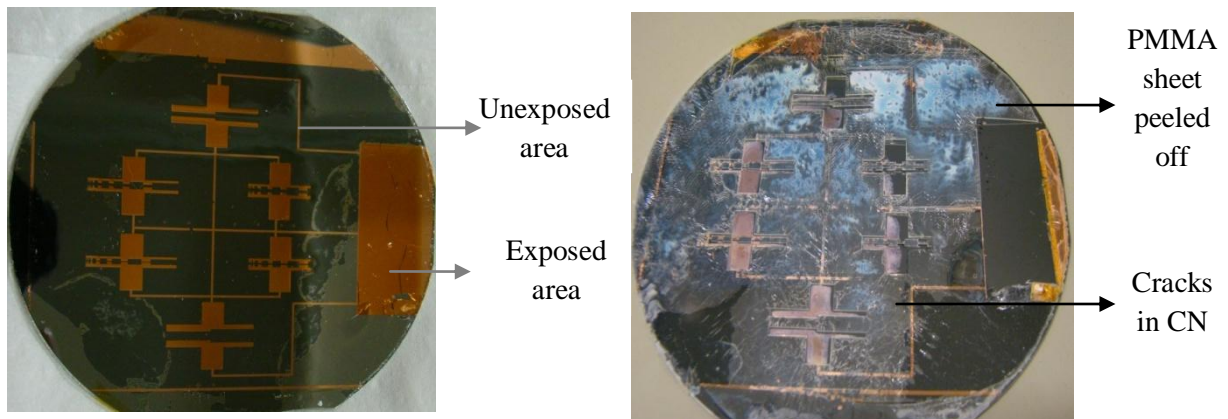


Fig11 (a) Sample after X-ray exposure, (b) Sample after development.

We found that the PMMA bonding was not proper as after development, PMMA sheet was peeling off and there are several cracks present in cyanoacrylate. Therefore further we have used different bonding method. This time we have taken Alumina wafer (57mm*57mm) which needs to be clean and dry before metal deposition. The surfaces must be free of dust, oil, fingerprint, grease or any other contaminants. The cleaning was done in an environment for clean room for optimal cleanliness. In literature the cleaning process uses chemical solutions containing hydrofluoric acid (HF), RCA and Acetone. RCA is mainly used for Alumina cleaning. In this process, TCE, and Acetone is used for cleaning and HF is used to remove the contaminants from the surface of the substrate by 10minute ultra-sonication in three separate steps. Finally wafer was rinsed off with DI water and dried with Nitrogen gas. After this we have sputter 100nm Cr and 400nm Ag onto it. As the size of the wafer is small therefore we are only making 3 devices out of 6 devices.

We spin coated PPR (AZ5214E) onto the wafer with the spin rate of 500rpm for 8sec and then 2000rpm for 45sec with the acceleration of 500rpm² which has given a thickness of ~2 μ m. To evaporate the solvent from the PPR, we prebake it at 100⁰C for 60sec. Now the sample is UV exposed at the UV intensity of 1.7mW/cm² for 20sec with the UV mask1 as shown in below figure7. We put the exposed sample in AZ726 MIF developer for 30sec then we rinsed the sample with DI water and dried with N₂. We etch Ag with HNO₃: H₂O=1:8 with the etch rate of 0.0697 μ m/min. For Cr etching, we have mixed 10.9gm Ceric Ammonium Nitrate, 4.25ml Per Chloric Acid and 84.85ml DI water. This solution etches Cr with the etch rate of

0.0667um/min. Next we dissolved the PPR with Acetone. Fig12 shows the images of the sample after each etching step.

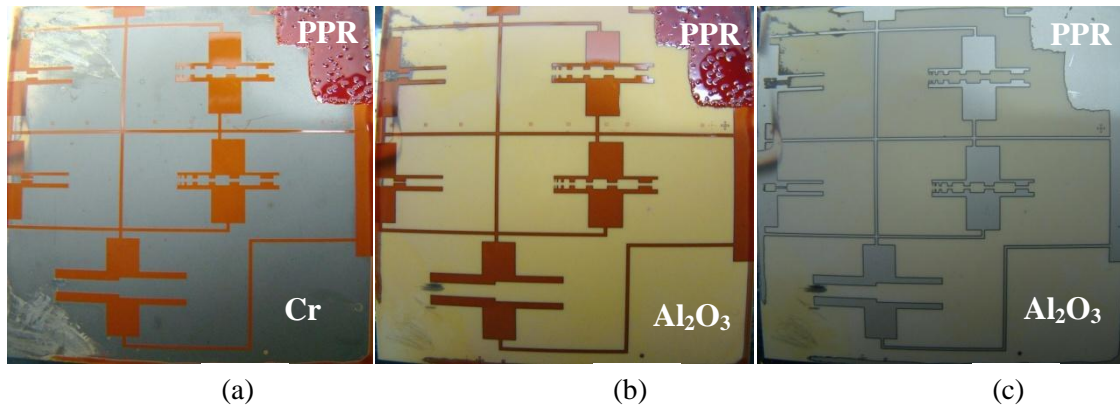


Fig.12 (a) Sample after Ag etching; (b) Sample after Cr etching; (c) Sample after dissolving PPR.

Now we have to bond 200um PMMA sheet to this wafer. First we have taken 0.5gm Methacryloyloxy propyle try methoxy silane (MEMO) and then mixed it with 23.5ml diluted Ethanol(Ethanol : H₂O=7:3). Next we titrated this solution with 99.98% acetic acid until the P^H value of the solution reaches 4.5 [5]. Further we call this solution as solution-A. 42.5gm Methyl Methacrylate (MMA) and 0.75gm Benzoyl peroxide (BPO) has been mixed together. Now we mixed solution-A into this solution and agitate it firmly for 30mins. After proper mixing we added 0.5gm Di-Methyl aniline (DMA) into this solution and mix firmly. By this paste, we bond the PMMA sheet with the wafer and applied a load of 0.15MPa for 13Hrs. PMMA bonded sample is shown in Fig13 (a).

The sample is now ready for X-ray exposure. First we align the X-ray mask-1 shown in Fig6 (a) with the sample and then exposed for 83,000Asec doses. After exposure, we put the sample in GG developer for 14Hrs and then in PMMA Rinser for 15mins. The sample is then rinsed with DI water and dried with N₂.

The sample is now electroplated with Ni. The electroplated area is 6cm². The electroplating has been performed at 70°C with the current density of 3A/dm² for 3hrs 20min. This will provide 200um thickness. The electroplated sample is shown in below fig13 (b).

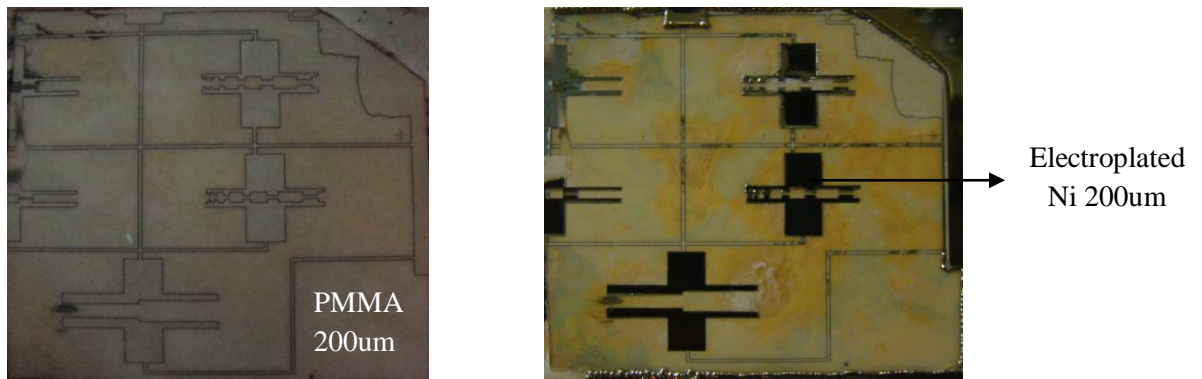
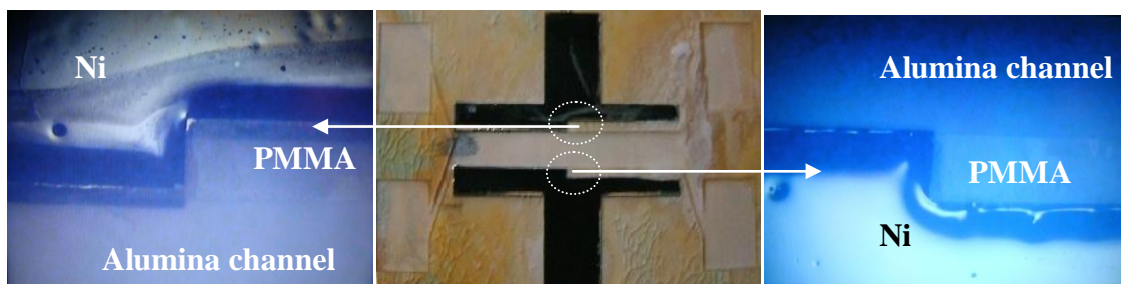
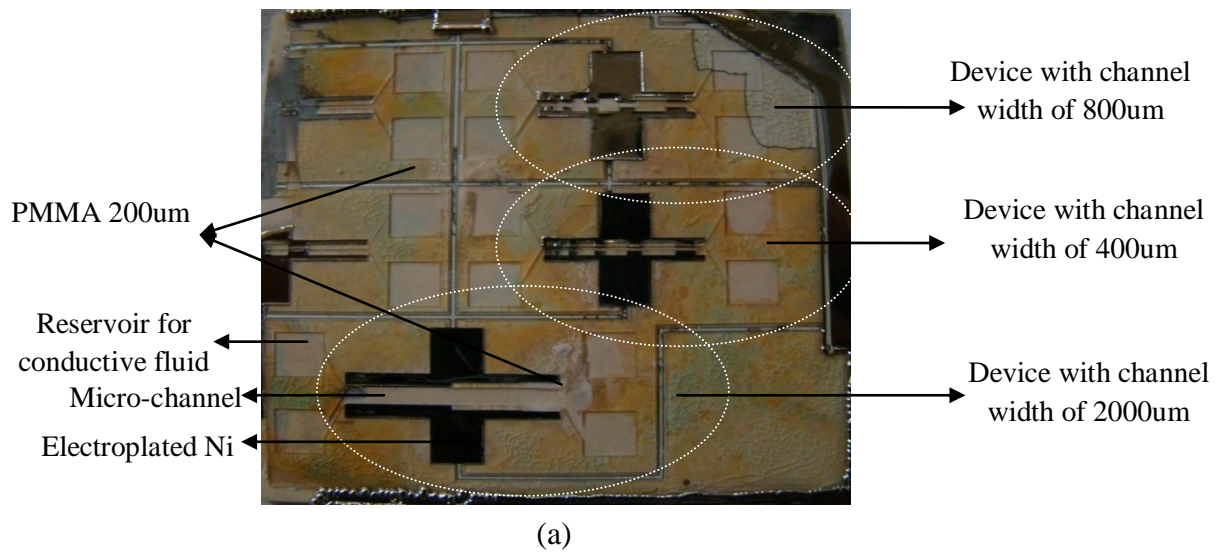


Fig.13 (a) Sample after PMMA bonding, (b) Sample after Ni electroplating.

Now we align X-ray mask-2 shown in fig6 (b) according to the sample and expose to provide 83,000Asec dose. After this we develop the sample with GG-developer for 14Hrs and then rinse it with PMMA rinser for 15mins. Further we separated out all three device structures. Below fig14 shows sample and its microscopic view.



(b)

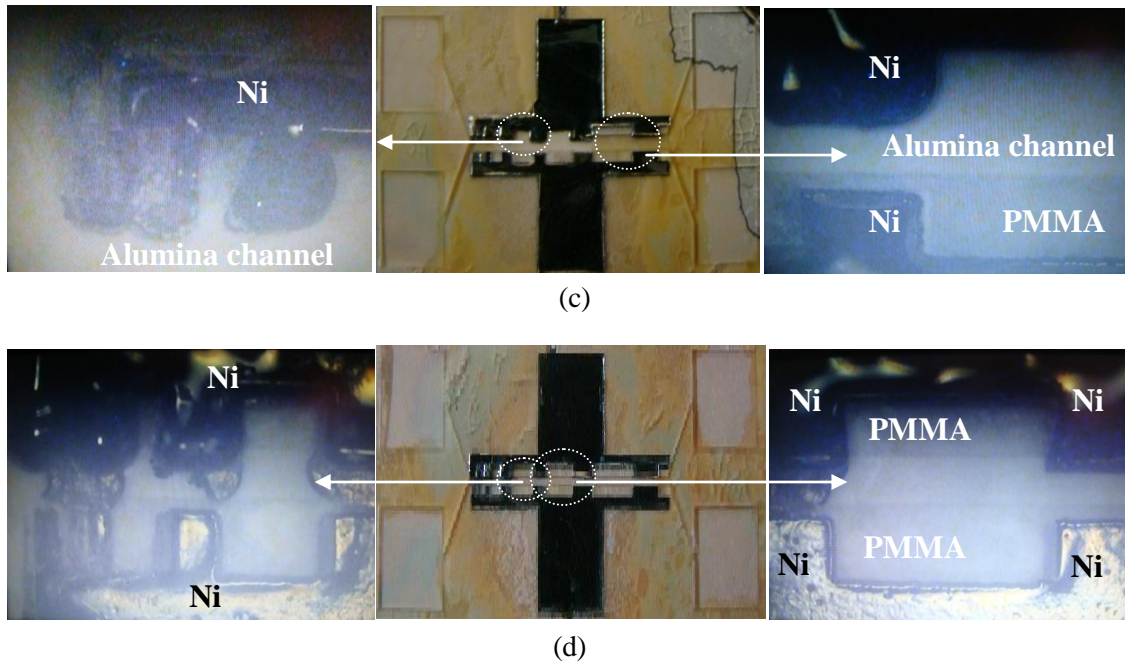


Fig.14 (a) Sample after development, (b) Device with 2000um channel width, (c) Device with 800um channel width, (d) Device with 400um channel width.

The Final task is to deposit dielectric layer but we have to protect contact pads from this deposition therefore we have done shadow masking of the contact pads through aluminum foil as shown in below fig15.

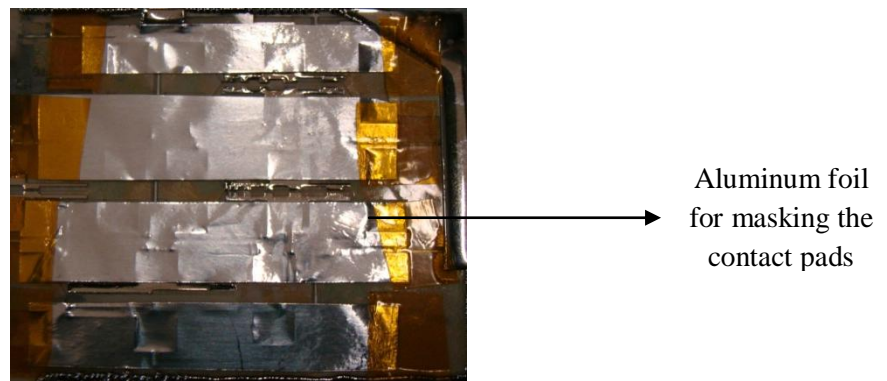


Fig15 Sample with shadow masking.

8.2 Device fabrication using UV lithography with Positive photoresist: Firstly Si wafer has been taken for standard RCA (RCA1: $\text{NH}_4\text{OH}:\text{H}_2\text{O}_2:\text{H}_2\text{O}=1:1:5$ at 80°C for 10mins; RCA2: $\text{HCL}:\text{H}_2\text{O}_2:\text{H}_2\text{O}=1:1:5$ at 80°C for 10mins) and Piranha cleaning ($\text{H}_2\text{SO}_4:\text{H}_2\text{O}_2 = 1:1$ for 10mins). After drying the wafer with N_2 , we sputter Ti and Cu of 50nm and 200nm respectively. Ti layer acts as a diffusion barrier layer for Cu and also improves the Cu adhesion with Si. We spin coated PPR (AZ5214E) onto the Si wafer with the spin rate of 500rpm for 8secs and then 2000rpm for 45secs with the acceleration of 500rpm² which has given a thickness of $\sim 2\mu\text{m}$. To evaporate the solvent from the PPR, we prebake it at 100°C for 60secs. Now the sample is UV exposed at the UV intensity of $1.7\text{mW}/\text{cm}^2$ for 20secs with the UV mask1 as shown in below figure7. We put the exposed sample in AZ726 MIF developer for 30secs then we rinsed the sample with DI water and dried with N_2 . Cu and Ti are now etched by Ammonium peroxydisulphate (APS=37g + 80ml water) at 40°C and HF: $\text{H}_2\text{O}_2:\text{H}_2\text{O}=1:1:20$ at room temperature respectively. After this we cleaned the sample with DI water and dried with N_2 . Fig.8 (a) shows the sample after etching.

On this sample, we spin coated thick PPR (AZ4903) at a spin rate of 500 rpm for 8 Sec and then 1000rpm for 60secs with the acceleration of 500rpm² which will give a thickness of 25 μm . Then we put the sample onto the hot plate at 100°C for 5min then waited till it acquired room temperature. After aligning UV mask2 with the sample, UV exposure has been performed onto the sample for 450secs with light intensity of $1.7\text{mW}/\text{cm}^2$. After this we develop the photoresist for 5mins in AZ400K developer (1:3) and dried the sample with N_2 . UV mask 2 and developed sample are shown in below Fig16.

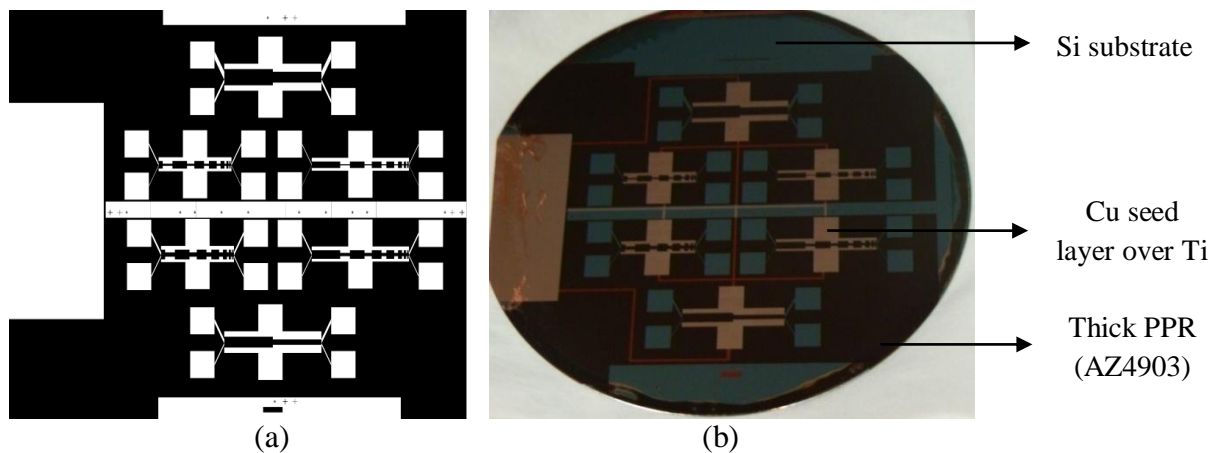


Fig16 (a) UV Mask2, (b) Sample after development.

Now Nickel (~25 μ m) has been electroplated onto this sample. Electroplating area is 0.13dm. Electroplating has been performed at 70°C with a current density of 3A/dm² for 25min. Ni electroplated sample is shown in Fig17.

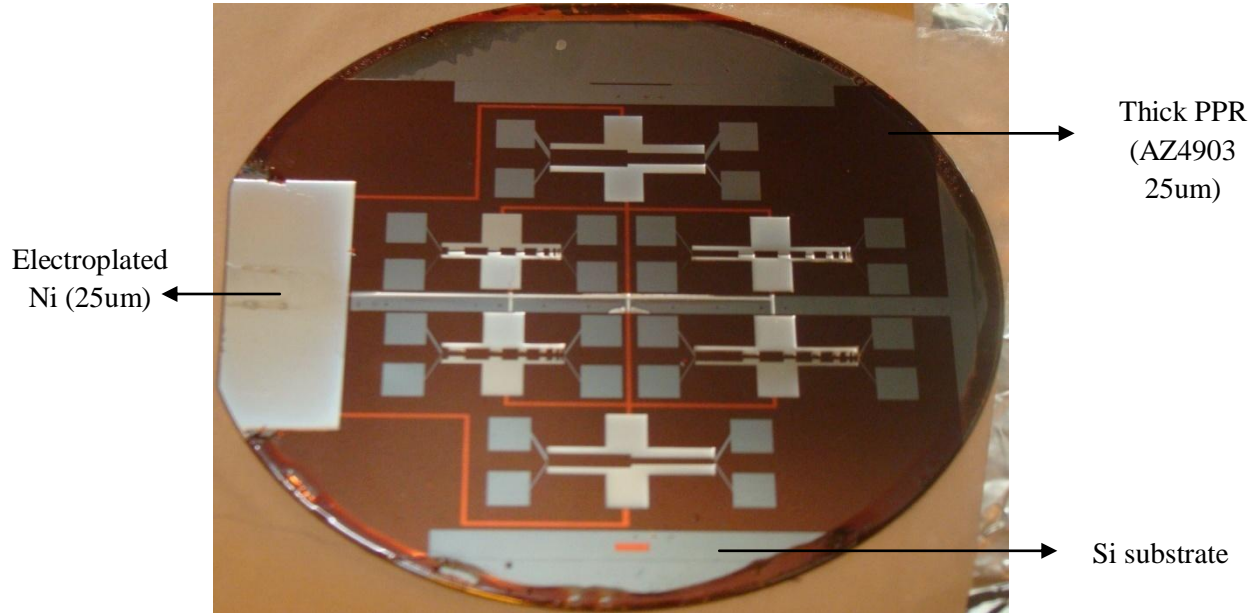


Fig.17 Ni electroplated sample.

We again aligned UV mask3 as shown below Fig.18 (a) with this sample and perform UV exposure for 110sec then we develop the sample with AZ400K (1:3) for 5min. After this we rinse the sample with DI water and dried it with N₂. Now the next step is to remove PPR from the channels and the contact lines. For doing so we have exposed the wafer with the mask shown in fig18 (b) then we developed the PPR with AZ400K developer for 5mins. After this we rinse the wafer with DI water and dried with N₂.

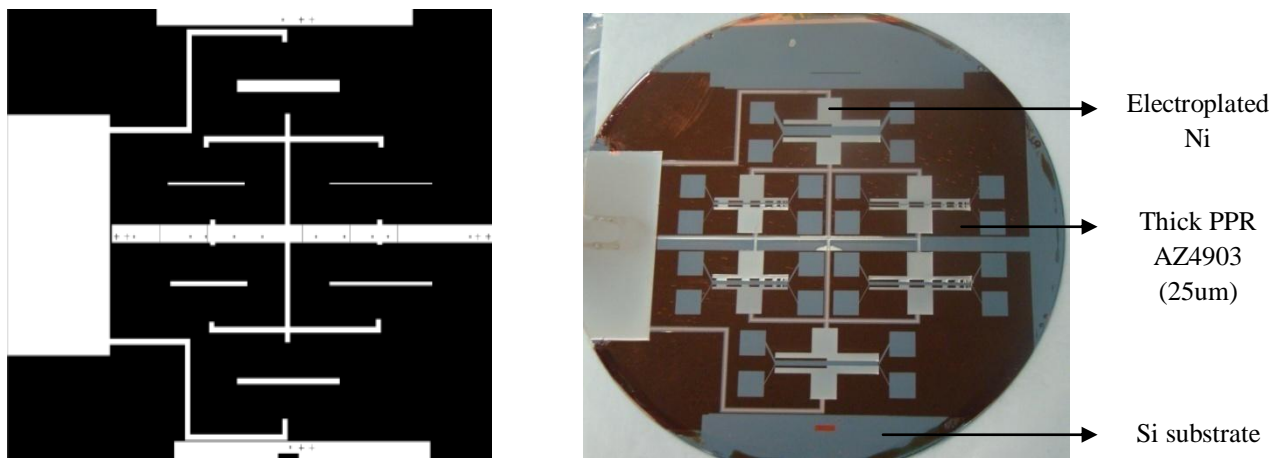
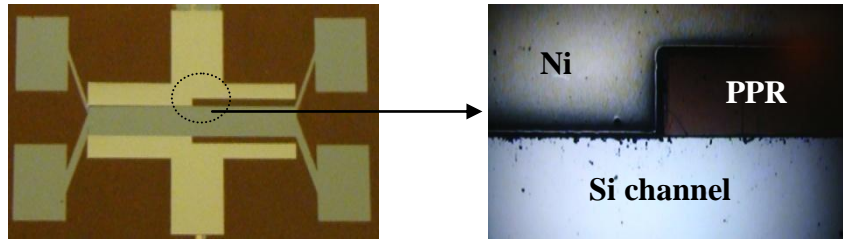
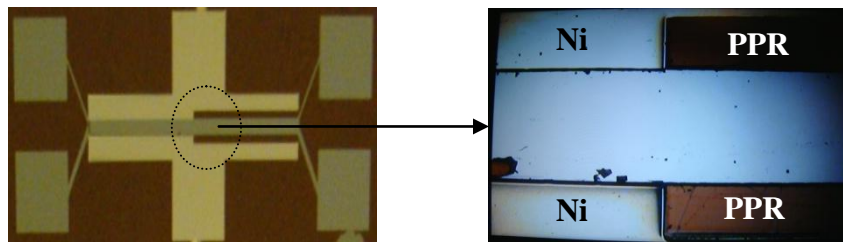


Fig.18 (a) UV mask3; (b) sample after removing PPR from channels and contact lines.

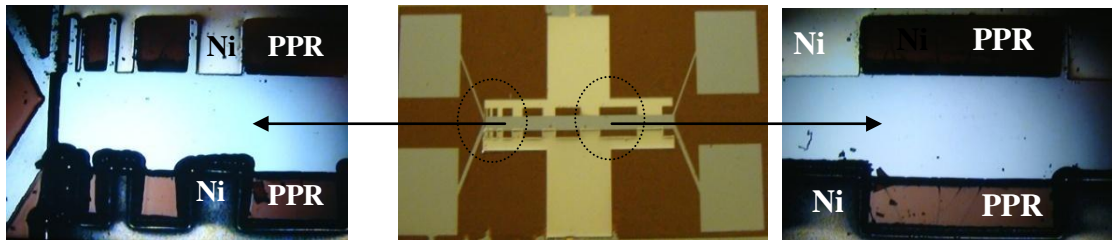
Now to isolate all the devices from each other we remove the contact lines. Below fig.19 shows all the individual devices and their Microscope images.



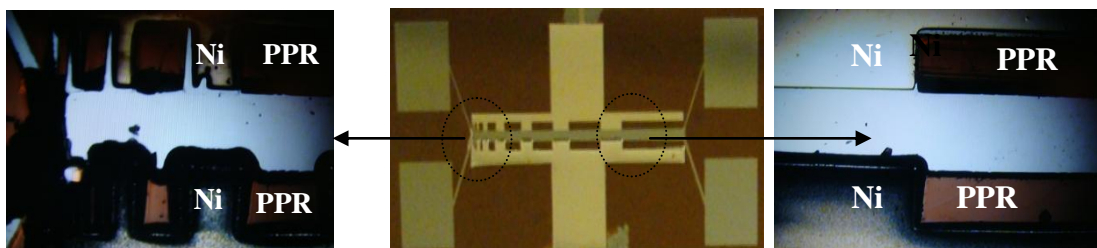
(a)



(b)



(c)



(d)

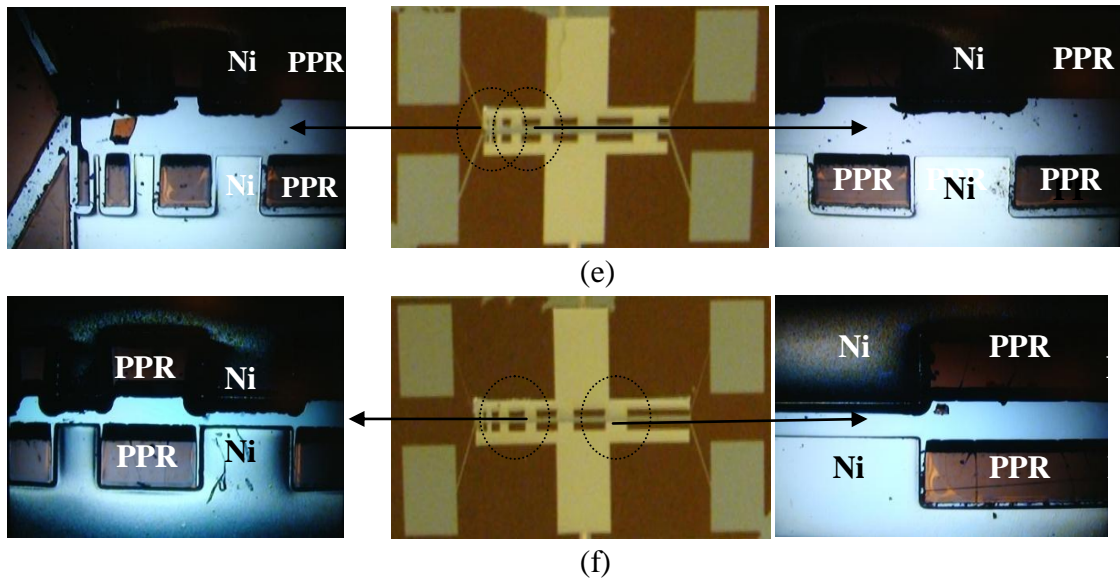


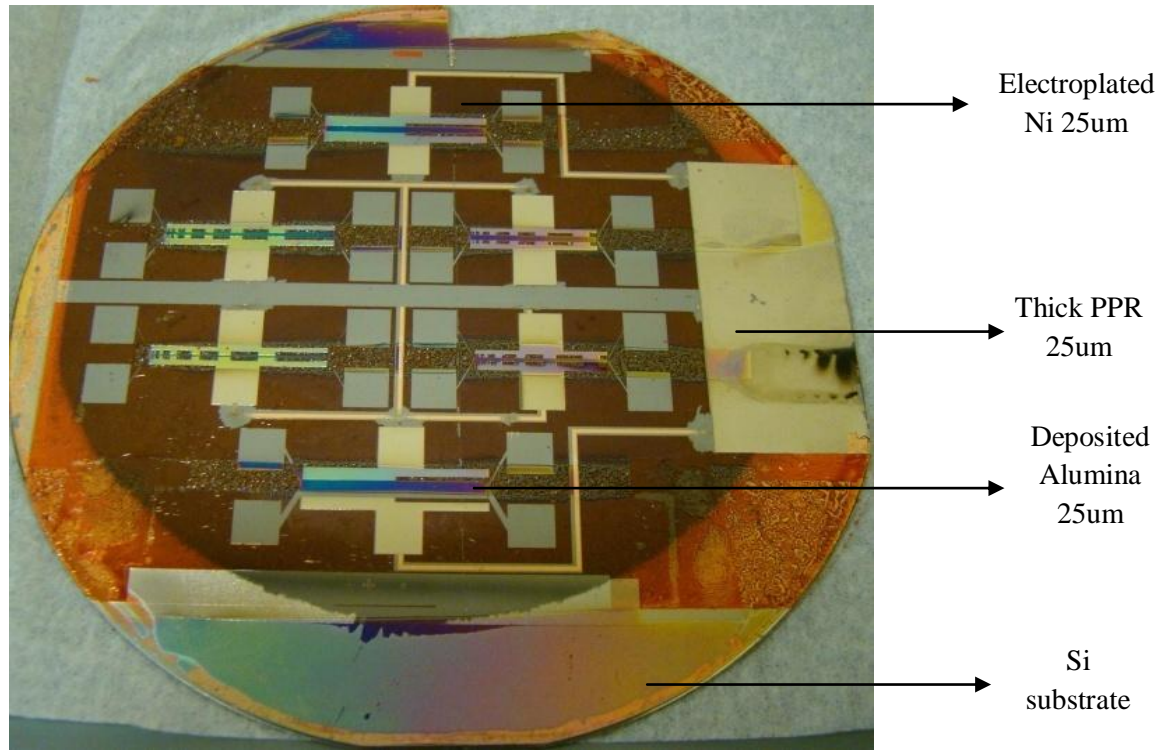
Fig19 (a) Device with 2000um channel, (b) Device with 1000um channel, (c) Device with 800um channel, (d) Device with 600um channel, (e) Device with 400um channel, (f) Device with 200um channel.

Further we have to deposit dielectric material onto the sample. We have chosen Alumina as a dielectric material because of its high dielectric constant. To protect contact pads from this deposition, shadow masking of the contact pads has been done as shown in Fig.20 (a). Fig.20 (b) shows the shadow masked wafer after alumina deposition.

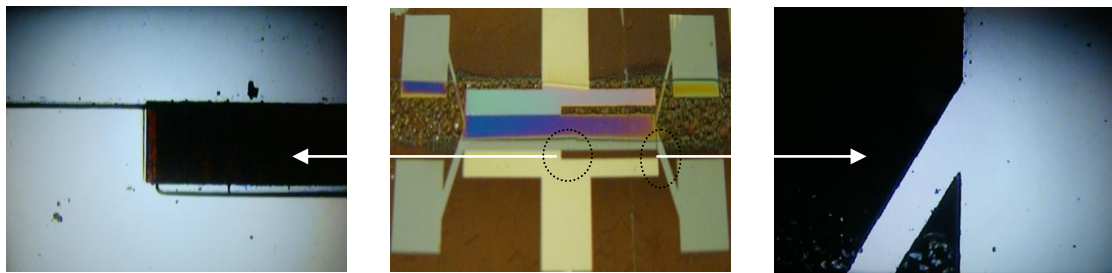


Fig.20 (a) Sample with shadow masking, (b) Alumina deposited sample.

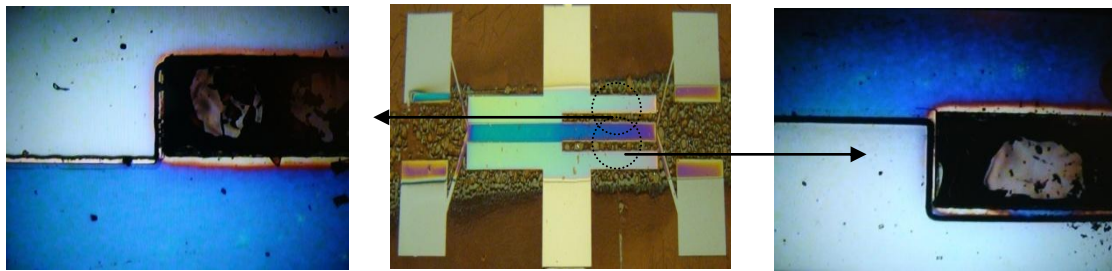
Below fig.21 shows the dielectric deposited sample (after removing shadow mask) and its microscopic views.



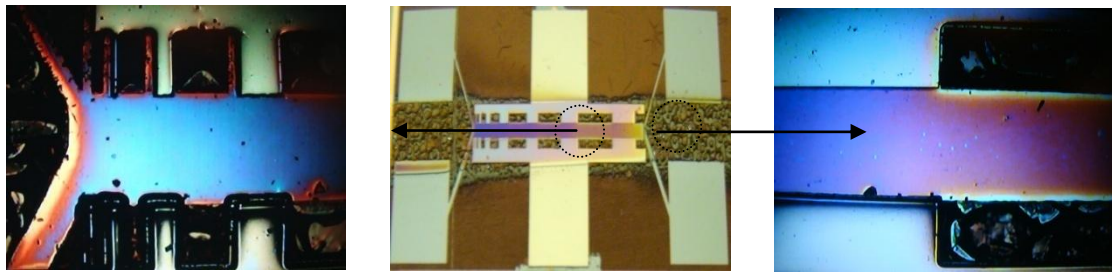
(a)



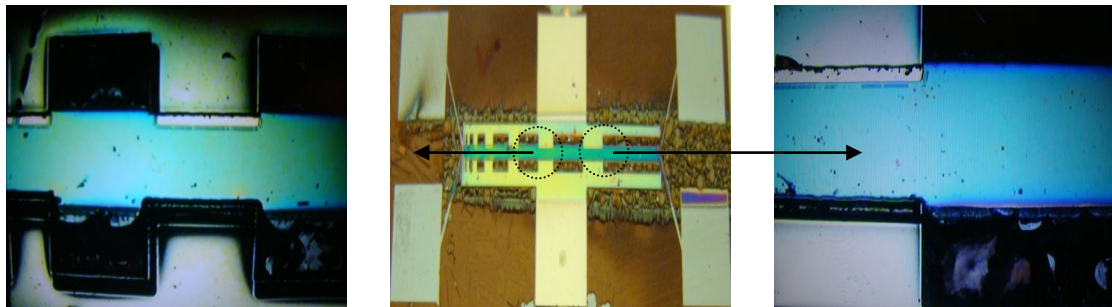
(b)



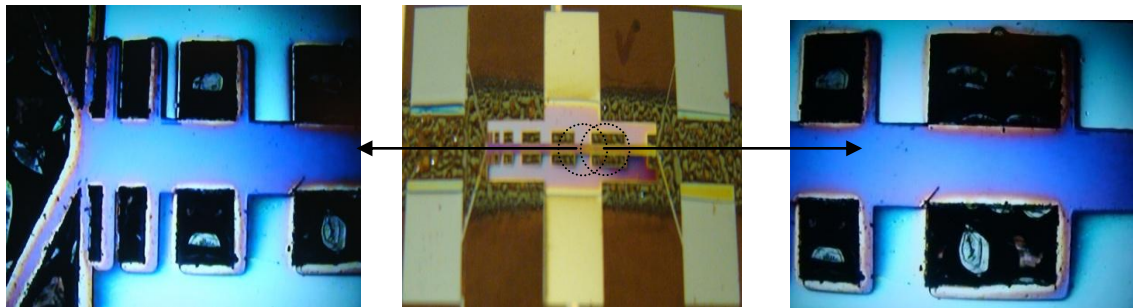
(c)



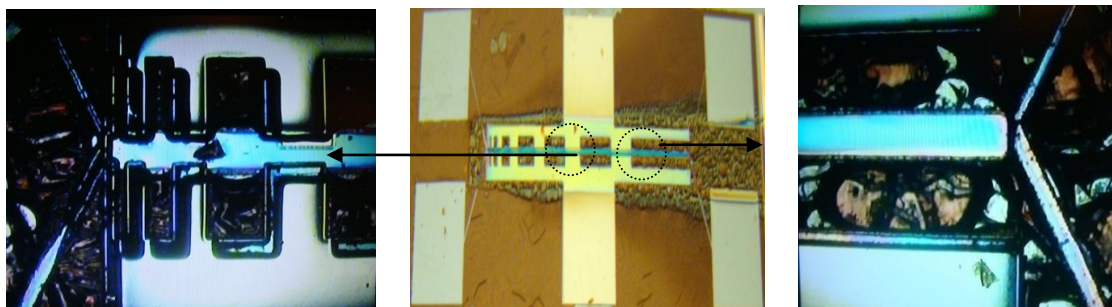
(d)



(e)



(f)



(g)

Fig.21 (a) Reverse electrowetting based energy harvesting device with channel width, (b) 2000μm, (c) 1000μm, (d) 800μm, (e) 600μm, (f) 400μm, (g) 200μm.

Finally, we cover the device with PMMA sheet. For doing so first we have cut 1mm thick PMMA sheet according to the size of the sample then we drill the sheet at some specific locations where contact pads and reservoirs have been located in the sample. We mix PDMS and its curing agent with 1:10 ratio and perform degassing. Further we spin coated this paste onto the PMMA sheet at 5000RPM for 60sec then we bond this PMMA sheet with the sample and baked it at 70C for 1Hr.

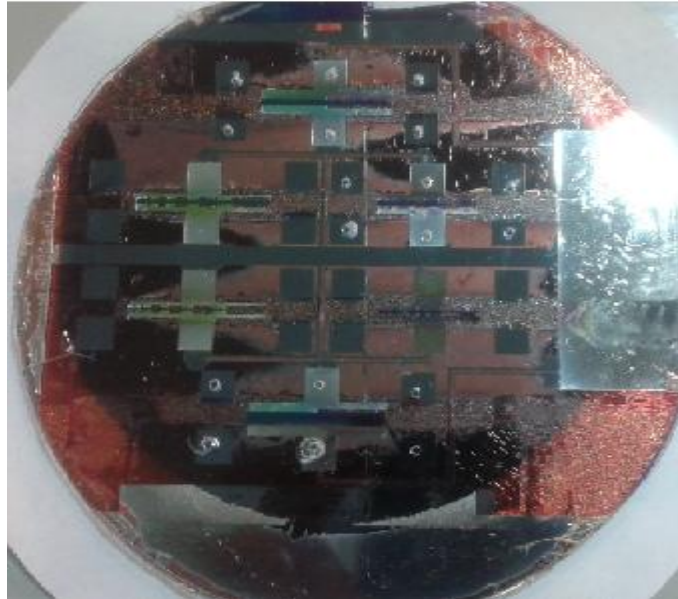


Fig.22 Reverse electrowetting based Eenergy harvester

8.3 Device fabrication using UV lithography with SU-8: Firstly Si wafer has been taken for standard RCA (RCA1: $\text{NH}_4\text{OH}:\text{H}_2\text{O}_2:\text{H}_2\text{O}=1:1:5$ at 80°C for 10mins; RCA2: $\text{HCL}:\text{H}_2\text{O}_2:\text{H}_2\text{O}=1:1:5$ at 80°C for 10mins) and Piranha cleaning ($\text{H}_2\text{SO}_4:\text{H}_2\text{O}_2 = 1:1$ for 10mins). After drying the wafer with N_2 , we sputter Ti and Cu of 50nm and 200nm respectively. Ti layer acts as a diffusion barrier layer for Cu and also improves the Cu adhesion with Si. We spin coated PPR (AZ5214E) onto the Si wafer with the spin rate of 500rpm for 8sec and then 2000rpm for 45sec with the acceleration of 500rpm^2 which has given a thickness of $\sim 2\mu\text{m}$. To evaporate the solvent from the PPR, we prebake it at 100°C for 60sec. Now the sample is UV exposed at the UV intensity of $1.7\text{mW}/\text{cm}^2$ for 20sec with the UV mask1 as shown in below figure7. We put the exposed sample in AZ726 MIF developer for 30sec then we rinsed the sample with DI water and dried with N_2 . Cu and Ti are now etched by Ammonium peroxydisulphate ($\text{APS}=37\text{g} + 80\text{ml water}$) at 40°C and $\text{HF}:\text{H}_2\text{O}_2:\text{H}_2\text{O}=1:1:20$ at room temperature respectively. After this we cleaned the sample with DI water and dried with N_2 . Fig.8 (a) shows the sample after etching.

Further we spin coated the sample with Omnicoat at a spin rate of 500RPM for 5sec and then 3000RPM for 30sec with the acceleration of 150RPM² but we found that it was non-uniform and even the adhesion was not good. Therefore to improve the adhesion before spin coated Omnicoat, we have spin coated a primer (HMDS). After this we baked the sample at 200C for 1min and waited till it acquired room temperature.

The next step is spin coat 2um thick SU8. For this we need to thin SU8 2025.

Resulting Volume (SU8 2002) =

$$\frac{\text{Solid content of available SU8 (SU8 2025)}}{\text{Solid content of Target SU8 (SU8 2002)}} * \text{Volume of available SU8 (SU8 2025)}$$

$$\text{Resulting Volume} = \frac{68.55}{29} * 20\text{ml}$$

$$\text{Resulting Volume} = 47.27\text{ml}$$

$$\text{SU8 thinner} = \text{Resulting volume} - \text{Initial volume}$$

$$= 47.27 - 20$$

$$= 27.27\text{ml}$$

So we have taken 20ml SU8-2025 and mixed 27.27ml SU8 thinner in it. Now we spin coat this solution onto the sample at a spin rate of 500RPM for 8sec and then 3000RPM for 45sec with the acceleration of 500RPM². We prebake the sample at 95C for 1min and then exposed it for 60sec at a light intensity of 1.7mJ/cm²sec using a mask shown below fig.23 (a) After this we post bake the sample at 95C for 1min and then develop it for 5mins. Below fig23 (b) shows the sample after development.

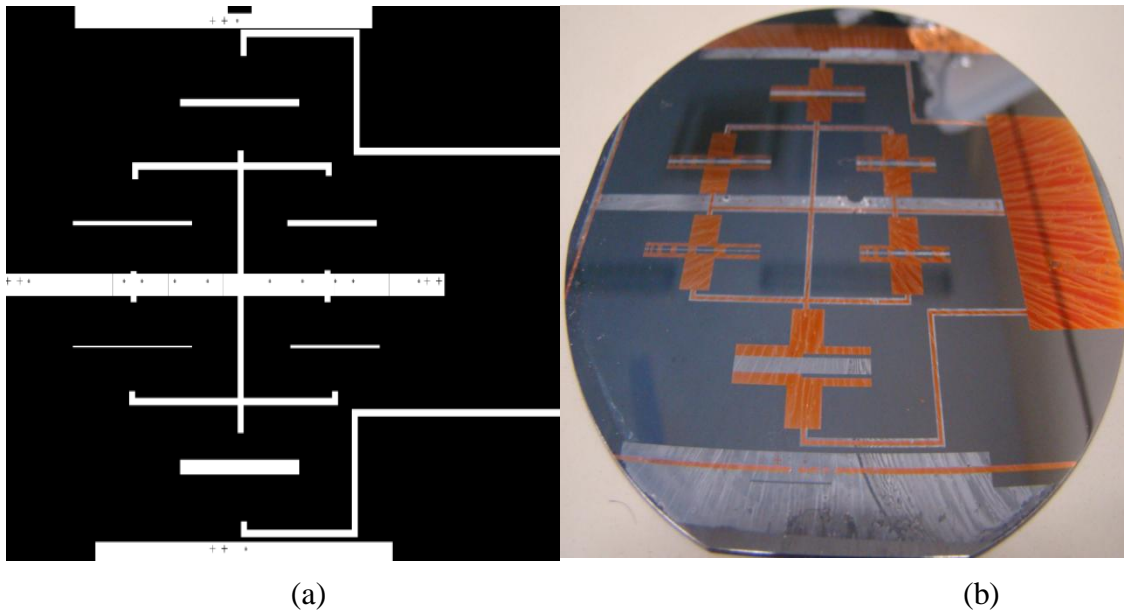


Fig23. (a) UV mask, (b) Sample after development.

Next we tried to dissolve omnicoat with Microposit MF319 but it didn't work. In the next attempt we reduce Omnicoat baking temperature to 120C and proceed with the previous procedure but on putting the sample in MF319, complete omnicoat get dissolved, even the omnicoat present under the exposed SU8 also get dissolved which peeled-off SU8 also as shown in below fig24.

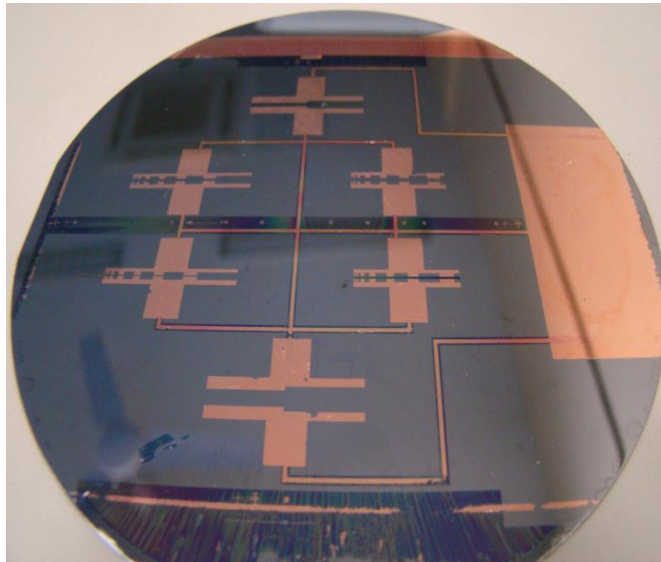


Fig.24 Sample after dissolving omnicoat.

This technique requires further optimizations but it seems that this technique is trustworthy to proceed.

8.4 Device fabrication without electroplating: Firstly Si wafer has been taken for standard RCA (RCA1: $\text{NH}_4\text{OH}:\text{H}_2\text{O}_2:\text{H}_2\text{O}=1:1:5$ at 80°C for 10mins; RCA2: $\text{HCL}:\text{H}_2\text{O}_2:\text{H}_2\text{O}=1:1:5$ at 80°C for 10mins) and Piranha cleaning ($\text{H}_2\text{SO}_4:\text{H}_2\text{O}_2 = 1:1$ for 10mins) then we put the wafer onto the hotplate at 200°C for 5 mins for dehydration and waited till it acquires room temperature. The first step is to form SU8 channels for this we have spin coated the wafer with SU8-2050 at 500RPM for 8sec and then 3000RPM for 45sec with the acceleration of 500RPM² which will give 50um thickness. To evaporate the solvent from the SU8, the sample is now prebaked at 65°C for 6mins and then 95°C for 10mins. Now the sample is UV exposed with the mask shown in fig25 (a) for 180sec with the intensity of $2\text{mJ}/\text{cm}^2\text{sec}$ then we post-bake the sample at 65°C for 1min and then 95°C for 8mins. The sample is now developed with SU8 developer for 6mins. After development we put the sample in IPA for 30sec if white fumes come it means that it is not developed yet, put again in developer. Finally after complete development we rinsed the sample with IPA and dried it with N_2 . The sample has been shown in fig25 (b).

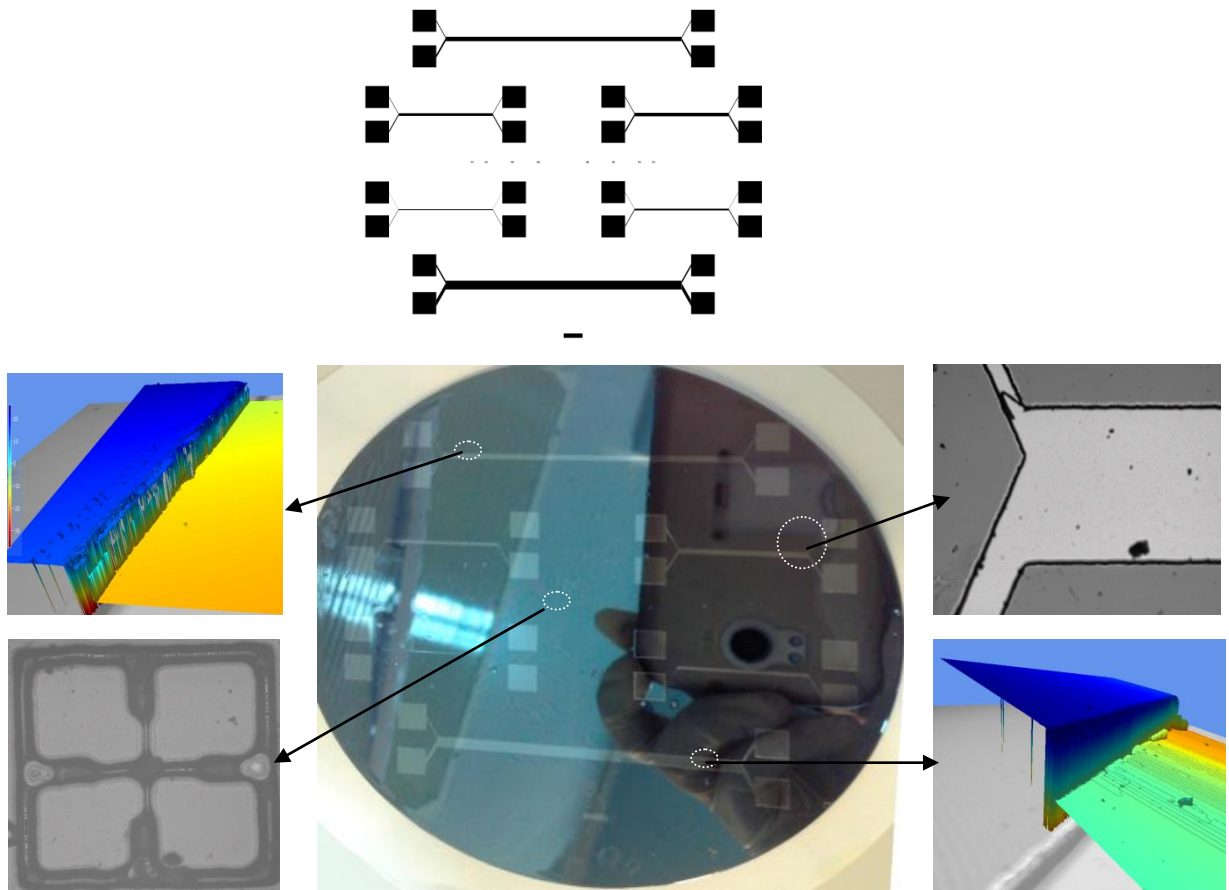


Fig25 (a) UV Mask1, (b) Sample after development and its microscopic view.

The next step is to form alternating electrodes in the SU8 side walls. For doing so first we have spin coated PPR (AZ5214E) at a spin rate of 500RPM for 8sec and then 2000RPM for 45Sec with the acceleration of 500RPM². This will give PPR thickness of 1.98um. Now to evaporate the solvents, we prebake the sample at 100C for 60sec then waited till it acquired room temperature. The sample is now exposed using the mask shown below fig.26 for 10sec with the UV light intensity of 17mJ/cm²sec. We put the sample in developer for 60sec then rinsed it with DI water and then dried it with N₂.

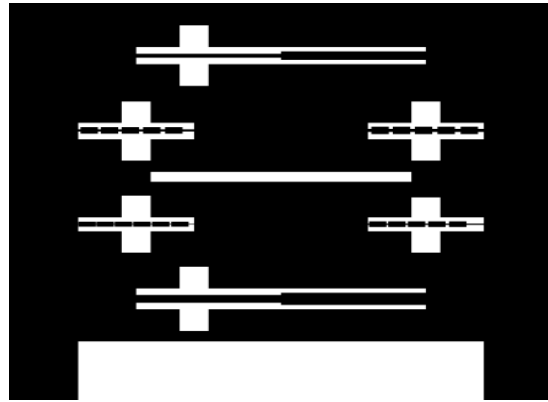


Fig26. UV mask2

After this, we have deposited 400nm thick titanium onto this sample using DC-sputtering for making side-wall electrodes. Now we put the sample in beaker filled with acetone and placed the beaker in sonicator for 5mins. Acetone will dissolve the PPR therefore the portion where PPR was present, Ti will Lift-off. Ahead, we rinse the sample with fresh acetone and DI water and dried with N₂.

Ideally we should have got alternating electrodes in the side wall of the channel but we didn't get. Then we tried to deposit Ti at 150C temperature by evaporator but this technique also didn't work. Aluminum has smaller atom size so we tried to deposit Al also at 150C using Evaporator but didn't work. Lastly we have tried to deposit Al at 150C with Tilt so that sidewall deposition should happen. First we deposited 400nm Al, making one side tilted then again we deposited 400nm Al making other side tilted but this technique also failed we were unable to get alternating electrodes in sidewalls of the channels. Below fig.27 shows the isometric view of the device by surface profile-meter.

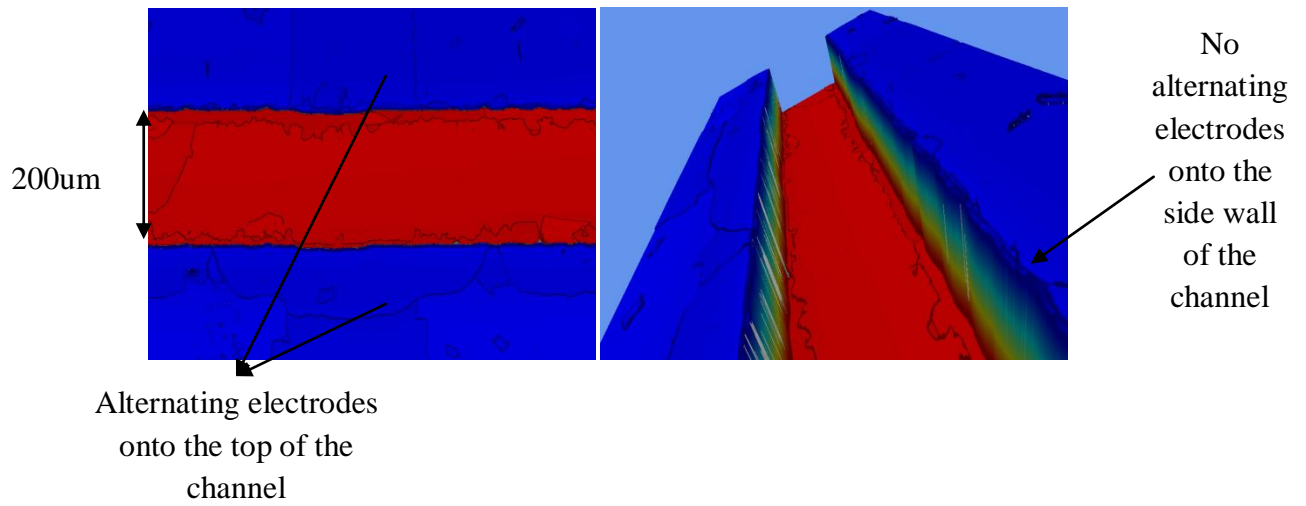


Fig 27(a) Top view, (b) Surface profilometer view

Finally we concluded that there is no problem in deposition but there is problem in UV lithography that is Patterning PPR in SU8 side-walls was the big problem. For making alternating electrodes onto the sidewall of the channels, first we should have opposite alternating PPR onto the sidewall of the channels. This was the biggest hurdle.

Conclusion and future work

Reverse-electrowetting based energy harvesting device simulation has been presented here along with several optimizations to increase the capacitance per unit volume at low operating voltage so that the device will be able to generate high energy. The device is offering maximum capacitance of 4.213nF at an operating voltage of 4.9V by optimizing dielectric material as titanium dioxide, dielectric thickness as 10nm and radius of device as 100 μ m.

Apart from device simulation, this energy harvesting device has been fabricated also by two different methods which need to be tested. Presently we have fabricated one droplet based device; in future we will use multiple droplets in the device so that the device capacitance would be very high and hence the generated energy. Use of multiple conductive droplets introduces the need of immiscible dielectric droplets which will be placed in between the conductive droplets. Galinstan and Polydimethylsiloxane (PDMS) can be a good choice for conductive and dielectric fluid respectively. Dielectric fluid doesn't participate in the actual operation of the device; it is just used to provide isolation between the conductive droplets therefore the volume occupied by these dielectric droplets reduces the capacitance per unit volume, offered by the device. In spite of this also, it is highly recommended to use multiple droplets for high energy harvesting. The power density of this energy harvester is very high and due to its fluidic nature, it offers very good environmental coupling which enables it to be used in various applications.

References

1. Krupenkin, T., Taylor, J. 2011. Reverse electrowetting as a new approach to high-power energy harvesting. *Nat. Commun.* 2:448.
2. Mugele, F., Duits, M. & van den Ende, D. Electrowetting: a versatile tool for drop manipulation, generation, and characterization. *Adv. Colloid Interface Sci.* **161**, 115 – 123 (2010).
3. E. O. Torres and G. A. Rincon-Mora, "Electrostatic Energy Harvester and Li-Ion Charger Circuit for Micro-Scale Applications," In proceeding of 49th IEEE International Midwest Symposium on Circuits and Systems, 2006, pp. 65 - 69.
4. J. Robertson, *Eur. Phys. J., Appl. Phys.* 28 (2004) 265.
5. V. K. P. Kanigicheri, K. W. Wally, E. Ma, W. Wang and M. C. Murphy, "Enhanced Adhesion of PMMA to copper with Black Oxide for Electrodeposition of High Aspect Ratio Nickel-Iron Microstructures," *Microsyst. Technol.*, **4**, 77-81, 1998.